CHALMERS
UNIVERSITY OF TECHNOLOGY

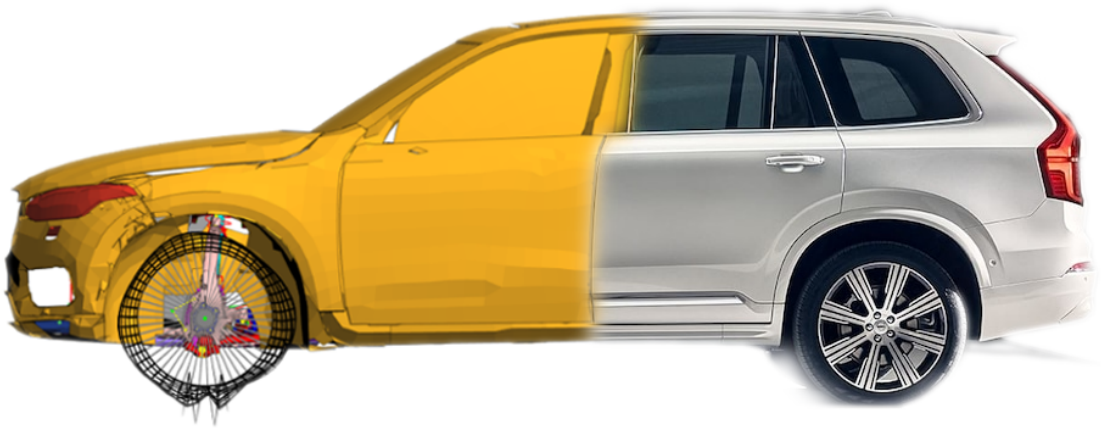

Tire modelling for cavity noise prediction in a complete vehicle simulation environment

Evaluation of CDTire/NVH in NVH Director

Master's thesis in Applied Mechanics

MAJA CARLSSON
DANIEL IDOFFSSON

Department of Mechanics and Maritime Sciences

CHALMERS UNIVERSITY OF TECHNOLOGY
Gothenburg, Sweden 2022
www.chalmers.se

Master's thesis 2022

Tire modelling for cavity noise prediction in a complete vehicle simulation environment

Evaluation of CDTire/NVH in NVH Director

MAJA CARLSSON
DANIEL IDOFFSSON

CHALMERS
UNIVERSITY OF TECHNOLOGY

Department of Mechanics and Maritime Sciences
Division of Dynamics
Chalmers University of Technology
Gothenburg, Sweden 2022

Tire modelling for cavity noise prediction in a complete vehicle simulation environment
Evaluation of CDTire/NVH in NVH Director
MAJA CARLSSON
DANIEL IDOFFSSON

Supervisors:
Dr. Jonathan Westlund, Volvo Car Corporation
Dr. Mathias Lidberg, Fraunhofer-Chalmers Centre for Industrial Mathematics

Examiner:
Prof. Thomas Abrahamsson, Dynamics, M2

Master's Thesis 2022:36
Department of Mechanics and Maritime Sciences
Division of Dynamics
Chalmers University of Technology
SE-412 96 Gothenburg
Telephone +46 31 772 1000

Cover: Volvo XC90 partly illustrated by a fem-model in NVHD and a photo of a physical vehicle.

Typeset in LaTeX
Printed by Chalmers Reproservice
Gothenburg, Sweden 2022

Tire modelling for cavity noise prediction in a complete vehicle simulation environment
Evaluation of CDTire/NVH in NVH Director
MAJA CARLSSON
DANIEL IDOFFSSON
Department of Mechanics and Maritime Sciences
Chalmers University of Technology

Abstract

With an ongoing transition in industry to battery electric vehicles, interior noise will no longer be dominated by an engine sound but shift to mainly originate from road noise instead. Road noise is highly dependent on the tires however traditionally used tire models have been insufficient in accurately predicting cavity noise which is problematic due to it being highly noticeable for the customer. New tire models have arised in recent years where CDTire/NVH is one of the most prominent ones. This thesis aims to evaluate the predictive capability of CDTire/NVH in the software package NVH Director (NVHD) but also conclude whether it can be advised or not to implement it in the working procedures at Volvo Car Corporation (VCC).

The evaluation was performed by comparing the performance of CDTire/NVH with the spindle load method as well as physical measurements. Primary focus of the comparisons were made on the complete vehicle, focusing on cavity noise in terms of predicted absolute values, trends and critical transfer paths. In addition to these comparisons, an evaluation of a stand alone tire were also made in order to capture the direct response.

Results show that CDTire/NVH in NVHD can capture the split of the cavity modes for a stand-alone tire but with unexpected sensitivity to the load case configuration. When implemented in the complete vehicle simulation model, there are ripples in the frequency response of interface forces. Furthermore, the transfer path analysis possibilities when using CDTire/NVH in NVHD is currently more restricted and fewer than the ones available with the spindle load method. All simulation results were obtained for one tire parameterization and simplified shaker excitation was used for the stand-alone tire. Due to the challenges encountered when adding the tires to the complete vehicle model in NVHD, it was neither possible to verify the performance of CDTire/NVH in NVHD by comparison with the established spindle load method nor possible to validate the tire model against full vehicle measurements. All results obtained in this thesis were obtained with NVHD version 21.2. Consequently, it is currently not advised to VCC to implement evaluated version of CDTire/NVH in NVHD into their working procedures. However, due to the potential of using CDTire/NVH in NVHD, it is also recommended to evaluate a revised version of the software addressing the issues identified in this thesis.

Keywords: CDTire, NVH, Road noise, Tire model, Hyperworks, Volvo Car Corporation

Acknowledgements

First, we would like to send our sincere gratitude towards our supervisor Dr. Jonathan Westlund for his support and guidance throughout the thesis project. Furthermore, we would also like to thank Patrik Ljungbäck & Joakim Truedsson at *Altair* for their valuable software support and our other supervisor Dr. Mathias Lidberg for additional feedback and support. We are also grateful for being warmly welcomed to the Road NVH team at Volvo Cars Corporation and a special thanks to Andre Passanesi for the help and guidance when conducting measurements.

Maja Carlsson, Gothenburg, June 2022
Daniel Idoffsson, Gothenburg, June 2022

List of Acronyms

Below is the list of acronyms that have been used throughout this thesis listed in alphabetical order:

BEV	Battery Electric Vehicle
CAE	Computer Aided Engineering
CRG	Curved Regular Grid
CSD	Cross Spectral Density
DOF	Degree Of Freedom
FEM	Finite Element Method
FRF	Frequency Response Function
FSI	Fluid Structure Interaction
ICE	Internal Combustion Engine
MBS	Multi Body Simulations
NTF	Noise Transfer Function
NVH	Noise Vibration and Harshness
NVHD	Altair's NVH Director
PNCS	Pirelli Noise Cancelling System
PSD	Power Spectral Density
SPL	Sound Pressure Level
VCC	Volvo Car Corporation

Nomenclature

Below is the nomenclature of parameters and variables that have been used throughout this thesis.

Parameters

$\Delta\omega$	Angular velocity step
Δf	Frequency step
Δx	Distance between two adjacent patch points
c	Speed of sound
N	Number of paths
R_0	Rim radius
R_{eff}	Effective radius
R_i	Tire radius
t	Time
v	Vehicle velocity

Variables

$\boldsymbol{a}$	Measured accelerations on knuckle
f_1	Lower cavity frequency
f_2	Higher cavity frequency
F_n	Operating force to path n
$\boldsymbol{F}$	Spindle forces at wheel center
$\boldsymbol{G_a}$	Cross spectral density matrix of accelerations
$\boldsymbol{G_F}$	Cross spectral density matrix of spindle forces
$\boldsymbol{G_P}$	Cross spectral density matrix of interface forces
$\boldsymbol{G_D}$	Cross spectral density matrix tire patch excitation
H_{mn}	Transfer function between point m and n

$\boldsymbol{H}_s$	Spindle frequency response function
$\boldsymbol{H}_v$	Chassis frequency response function
$\boldsymbol{H}_T$	Tire patch frequency response function
L	Length of waveguide
$\boldsymbol{P}$	Interface forces
$\boldsymbol{S}_X$	Power spectral density matrix of response
y_m	Sum of contributions at location m
y_n	Partial contribution from path n

Contents

List of Figures

List of Tables

1

Introduction

1.1 Background

When driving a vehicle, the noise and vibrations play a major part in how the quality is perceived. With an ongoing transition in industry from *Internal Combustion Engine*s (ICE) to *Battery Electric Vehicles* (BEV), road noise will be of even greater importance as it no longer will be masked by an engine sound. Road noise can be of two different types, airborne and structure-borne, where the latter one is dominant up to around 400Hz. Structure-borne noise is transferred by excitations from the road through the vehicle structure, causing vibrations which in turn emits noises. Previously, structure-borne noise was mainly dominated by engine excitations, yet with a significant impact from road noise as well. However, with BEV:s this will shift to mainly be dominated by the latter one.

Road noise is highly dependent on the interaction between tire, rim, road and body structure. Commonly this is treated numerically by using the *Finite Element Method* (FEM), where the analysis is based on excitation using measured spindle loads from physical tests. The drawbacks with this method is that it bypasses the tires which excludes them from analysis and that it requires a complete physical vehicle. Furthermore the measured excitation is highly individual and cannot be transferred to other configurations as the assembly of wheels and suspension is strongly coupled. In spite of that, the method is widely used since existing finite-element tire models has not been sufficiently good or supported in the software.

Traditionally used tire models have been insufficient in accurately predicting the *Fluid Structure Interaction* (FSI) between the air cavity and the tire & rim structure. Due to this, cavity noise which occurs in the range of 160-220 Hz has not been accurately predicted. This is problematic due to the tonality of cavity noise that can be highly noticeable for the customer and thereby the perception of the car's quality. However, in recent years new tire models have emerged that are detailed enough for accurate *Noise, Vibration & Harshness* (NVH) predictions over the whole frequency band for structure-borne road noise. Out of these the *Comfort and Durability Tire* (CDTire) model, developed by Fraunhofer ITWM, is a prominent one.

1.2 Aim

The aim of this thesis is to evaluate the predictive capability of a CDTire/NVH model within the area of road NVH. Furthermore, the thesis aims to conclude whether it can be advised or not to implement CDTire/NVH into existing working procedures at *Volvo Car Corporation* (VCC). By using a CDTire/NVH model, predictions will be based on actual road surface data rather from vehicle measurements, hence enabling fully simulation-based analyses of the vehicle. With accurate predictions in the development stage of a car, early focus can be put on critical components and areas to improve.

1.3 Objective

The thesis will be carried out at VCC and implementation of the CDTire/NVH model will be made in *Altair's NVH Director*, henceforth called NVHD, using an existing complete FE vehicle model. In order to validate its capability, CAE results using both CDTire/NVH as well as spindle loads will be compared to obtained measurement data. The comparison will primarily focus on responses at frequencies in the cavity region and will be made in terms of predicted absolute values, trends and critical paths using transfer path analysis. Additionally, a separate delta study using two different tire pressures will be performed, comparing the predicted differences between the methods.

1.4 Delimitations

The project concerns one unique tire setup as well as one specific car model, *Pirelli PZERO 275/35 R22* without *Pirelli Noise Cancelling System* (PNCS) and Volvo XC90 B6 AWD. One specific road surface will be used for the physical test and simulations, Barfield road at Hällered proving ground. Further testing with different tire setups, car models as well as other road surfaces are not in the scope of this project and is left as future work. In addition, enveloping of scanned road surface data is not investigated in this report. The analysis will concern the different complete vehicle models' ability to predict interior noise in the frequency range of 60-300Hz. Within this interval, primary focus will lie on cavity noise in the range 160-220Hz.

1.5 Related work

In similarity to the purpose of this report, there are other publications made within almost the same area of focus. While this thesis focuses on the implementation of the CDTire/NVH model and its validity in comparison to current NVH prediction approaches in the cavity noise range, other publications have a slightly different purpose. Judging by the number of reports within the topic, it appears that it is still a quite rarely used model in industry. Nevertheless, a general summation of the

reports suggest that the CDTire model has a good capability of making accurate NVH predictions.

The fundamental idea of Uhlar and Kunicky [2020] is the procedure of combining *Multi Body Simulations* (MBS) and FEM when predicting structure-borne noise. Instead of using acceleration measurements on the hub, which can be transferred into reaction forces, nor rely on a complete finite element software, the authors use a so-called hybrid simulation approach. The idea behind this approach is the reliance on both the FE-models for calculating the body structure and interior noise but also the use of a MBS procedure to capture non-linearities.

As mentioned by the authors, that is not a unique solution for a problem of that kind. However, within the area of taking the tires into account with frequencies up to 250 Hz, this is a new way of approaching the problem. Not only the combination of MBS and FE, but also the implementation of an appropriate tire model, which in this case is CDTire. One benefit mentioned is the possibility of investigating influences from different parameters and characteristics of the tires. Another one is the improved ability for collaboration between departments at early development stages.

In Uhlar et. al. [2019], which is also used as a reference in Uhlar and Kunicky [2020], the objective is to compare the two commercial physical tire models, CDTire and FTire, in a frequency range of 0-300 Hz. Written by the authors themselves, there were at this time no other independent comparison of the two models in the area of NVH analysis for frequencies above 100 Hz. Unlike the previously mentioned publication, the focus in this report is a comparison of the two models against each other, rather than how they could be used in analyses.

The comparison was performed by comparing forces obtained using MBS in MSC .ADAMS with measurements made in a test rig with both a cleat impact and a rough road surface. Judging by the results obtained in the tests, the CDTire showed a more consistently high performance in capturing the structural dynamics and the force amplitude than the FTire model. In particular, CDTire were able to capture the modal behavior in the air cavity regions at around 200 Hz which FTire had difficulties with. A final remark made by the authors was that both tire models neglect the dynamics of the rim which in their sense would be a necessary aspect to improve in order to have more reliable results in the cavity region.

In Gallrein et. al. [2018], CDTire's capability of capturing the air cavity oscillations are being tested and compared against measured values. In similarity to Uhlar et. al. [2019], the test data were obtained using a test rig with a cleat impact. The purpose of the report is to prove the necessity of having a dynamic gas equation included in the CDTire model in order to capture cavity modes. By comparisons against measurements, it is shown that the compressible Euler cavity model is the only cavity model that can capture the modal behavior for frequencies above 200 Hz.

These reports claim great potentials of using the CDTire model, both in terms of its predictability and the beneficial collaboration and development possibilities. However, this project differs in procedure compared to the previous work just described. Unlike the previous work, focus of this thesis will be more strictly at the cavity region with actual road surface as input, but also evaluate using NVHD, which will be presented in the following chapters.

2

Theory

This chapter presents important theories and elements that will be used later in the report. The fundamentals of road noise, spindle load measurements and the CDTire model are presented.

2.1 Road noise

Road noise has two paths to propagate from tire-road contact to noise in the passenger cabin, through the structure and the air. As mentioned in Section 1.1, structure-borne is the dominating one below 400Hz while airborne dominates for frequencies above that. Within the structure-borne range the main mechanism causing radiated noise is the vibrations generated by the tire-road interaction between the tread blocks and road surface.

This is complex to model as it consists of a multi-source, nonlinear excitation due to the interaction between road and tire followed by long vibration paths through the vehicle chassis into the interior. The noise can be divided into different subtypes, with separate tonality and frequency ranges where they are the most distinguished. The frequency region where structure-borne noise is dominant can be divided into drumming, rumble, tyre cavity and rough tyre types of noise. Out of these 4, cavity noise has proven to be the most difficult one to predict due to the complexity of the FSI between the tire structure and the acoustic modes in the cavity.

2.1.1 Cavity noise

Tire cavity noise is a problematic sound due to the resonance of enclosed air within a tire itself. The sound can be highly noticeable and occurs as two narrow but distinct peaks which vary with tire dimension, temperature and vehicle speed. This section will briefly describe the cavity theory according to O'Boy [2020] which the reader is encouraged to read for further information.

The tire geometry can be estimated as a cylindrical annulus where the pressure perturbation is assumed to vary along the radial and circumferential position, but invariant in the axial direction. In terms of the actual tire, this means that the

width is not a dependent variable when dealing with cavity resonances.

When the air at the contact patch is excited by tread rubber movement, it excites a number of cavity modes. The first mode, which corresponds to the air moving up and down within the tire, yields a varying force on the wheel hub. This generates structure-borne vibrations which in turn results in interior noise. Further on, it has been shown that the second and the third acoustic modes cancel each other, hence they have no influence on the net force.

In the case of an unloaded tire without rotation, the air cavity will result in two twin modes. This is due to the equal wave travel length of the enclosed air. When the tire instead is loaded or set into rotation, a split of the two frequencies appear. This is due to induced asymmetry if loaded, or due to the Doppler shift effect if rotating, which affects the speed of the wave in the tire cavity. The speed of the forward circumferential acoustic wave at the trailing edge is reduced by the vehicle velocity v while the backward travelling wave at the leading edge is increased by the corresponding value. An estimation of the cavity frequencies f_1 and f_2 can be made according to Equation 2.1.

$$f_1 = \frac{(c - v)}{L} \qquad f_2 = \frac{(c + v)}{L} \tag{2.1}$$

where c is the speed of sound and L is the length of the waveguide described by Equation 2.2

$$L = 2\pi R_{eff} \tag{2.2}$$

and the effective radius R_{eff} being estimated by the average of the rim radius R_0 and the overall tire radius R measured as the outer radius in the center of the tread according to Equation 2.3.

$$R_{eff} = \frac{(R_0 + R)}{2} \tag{2.3}$$

Since the speed of sound is temperature dependent, it follows that $f_i = f_i(T, R_{eff}, v)$, $i = 1, 2$.

2.2 Transfer Path Analysis

Transfer Path Analysis (TPA) is a method to identify key contributors to a vibration or noise problem and rank them by their impact. The theory presented in this section is based on Cinkraut [2015] which the reader is referred to for a more comprehensive reading.

The technique provides useful information for in depth analysis of noise and vibration propagation. It breaks down the problem using source loads and transfer functions to the targeted receiving locations. Transfer functions tell how the loads propagate from the source to the targeted location where the noise or vibration is perceived.

One example of a load source are impact forces acting on the wheel hub. This analysis technique is valid for linear, time-invariant systems.

The target location, for example sound pressure at a given receiver location in the interior of the car, can be defined as a sum of contributions of partial sound pressures. In Equation 2.4, $y_m(\omega)$ is the total sound pressure level at receiving point m and $y_n(\omega)$ represents the partial contribution from path n out of total number of paths N.

$$y_m(\omega) = \sum_{n=1}^{N} y_n(\omega) \tag{2.4}$$

The partial contributions $y_n(\omega)$ are defined as the excitation force $F_n(\omega)$ in the given path multiplied with the transfer function H_{mn}, which results in $y_m(\omega)$ expressed according to Equation 2.5 below.

$$y_m(\omega) = \sum_{n=1}^{N} H_{mn} F_n(\omega) \tag{2.5}$$

where H_{mn} is the transfer function between point m and path n and $F_n(\omega)$ is the operating force to path n.

An example of transfer paths in a car's front wheel suspension is visualized in Figure 2.1, starting from an excitation source and transferring via different paths to a final receiving location. In this example the starting point is excitation at the wheel center and receiving locations are two interface points, 109 on the upper link arm and 102 on the subframe attachment to the body.

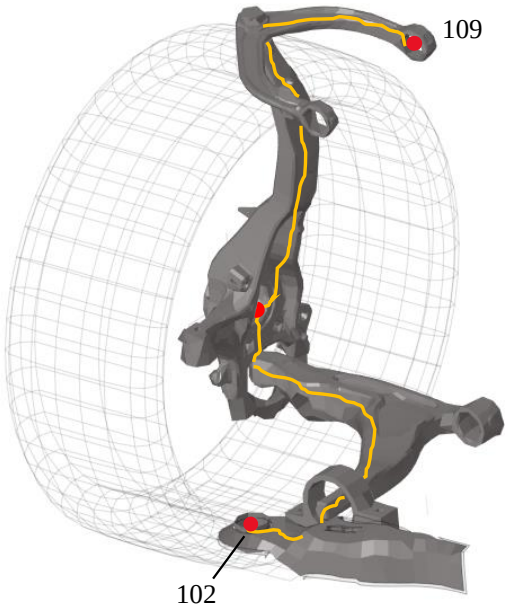

Figure 2.1: Example of a transfer path in the front wheel suspension where excitation propagate from wheel hub to receiving points 102 and 109.

With TPA, a DNA plot can be generated. A DNA plot is one way to represent the results obtained by the TPA. It ranks the contributions from the interface points for a given range of frequencies, enabling an easy overview of which paths contributes the most. It also visualizes how the contributions vary for different frequencies, enabling to identify the sources of different peaks occurring throughout the frequency range.

2.3 Spindle load measurement

The spindle load method is a way to bypass the need of accurate tire models when performing road NVH analyses. This is done because of the difficulties to model tires due to the FSI, rim dynamics and gyroscopic effects. The method, which is further described in Park et. al. [2001], is based on measured accelerations $\mathbf{a}(\omega)$ at four points per knuckle using three-dimensional accelerometers. In total, this results in 48 different signals. The translation from accelerations at the knuckle positions into spindle forces at the wheel center $\mathbf{F}(\omega)$ can be described according to Equation 2.6:

$$\mathbf{a}(\omega) = \mathbf{H_s}(\omega)\mathbf{F}(\omega) \tag{2.6}$$

where $\mathbf{H_s}(\omega)$ denotes the spindle *Frequency Response Function* (FRF). Henceforth, since all matrices are frequency dependent, ω will not be printed out as the independent variable. The spindle forces are assumed to be excited in five of the six possible *Degrees Of Freedom* (DOF):s, the translational directions seen in Figure 2.2 and rotation around the x- & z-axis. The assumption is based on the fact that there is no moment around the rotating y-axis to consider. As a consequence of this, $\mathbf{H_s}$ results in a non-square matrix (48×20).

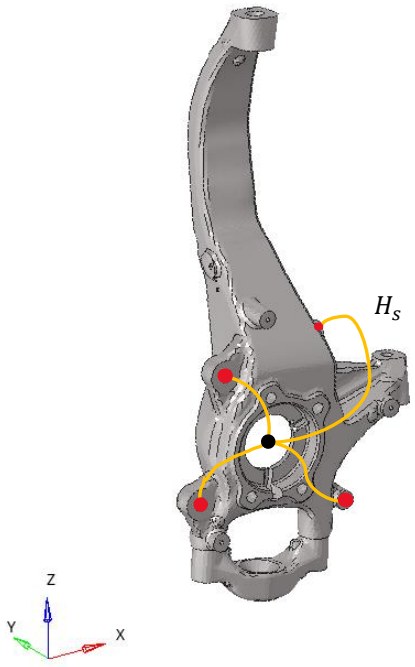

Figure 2.2: Knuckle with illustrated spindle frequency response function.

From Equation 2.6 it follows that the *Cross Spectral Density* (CSD) matrix $\mathbf{G_a}$ of the accelerations can be described as following in equation Equation 2.7:

$$\mathbf{G_a} = \mathbf{H_S} \mathbf{G_F} \mathbf{H_S^H} \tag{2.7}$$

where $\mathbf{G_F}$ denotes the CSD matrix of the spindle loads. Due to the non-square dimension of $\mathbf{H_s}$, $\mathbf{G_F}$ can be estimated using pseudo-inversion in Equation 2.8:

$$\mathbf{G_F} = \mathbf{H_S^+} \mathbf{G_a} \mathbf{H_S^{+H}} \tag{2.8}$$

where $[\cdot]^H$ and $[\cdot]^+$ denotes the Hermitian transpose and Moore-Penrose pseudo-inverse respectively. For a known spindle load $\mathbf{F}$, the corresponding interface forces $\mathbf{P}$ can be estimated using the chassis FRF $\mathbf{H_V}$ as Equation 2.9:

$$\mathbf{P} = \mathbf{H_v} \mathbf{F} \tag{2.9}$$

where the interface forces refers to the forces on the vehicle body at the interface between the chassis and the body. Since the dimension of $\mathbf{P}$ depends on the number of interface response forces, N, it also affects the size of $\mathbf{H_v}$ ($N \times 20$). Hence, the corresponding CSD-matrix is obtained according to Equation 2.10:

$$\mathbf{G_P} = \mathbf{H_v} \mathbf{G_F} \mathbf{H_v^H} \tag{2.10}$$

The RMS-value of an interface force P_j for a defined frequency step $\Delta\omega$ is then obtained by taking the square root of the CSD-matrix $\mathbf{G_P}$ according to Equation 2.11:

$$\begin{aligned} P_j(\omega - \delta\omega, \omega + \delta\omega) &= \sqrt{\frac{1}{2\pi} \int_{\omega-\delta\omega}^{\omega+\delta\omega} G_{P_{jj}}(\omega) d\omega} \\ &\approx \sqrt{\frac{1}{2\pi} G_{P_{jj}}(\omega)[(\omega + \delta\omega) - (\omega - \delta\omega)]} \\ &= \sqrt{\frac{1}{2\pi} G_{P_{jj}}(\omega) 2\delta\omega} \\ &= \{\text{For frequency step } \Delta f = 1 \rightarrow \Delta\omega = 2\pi\Delta f = 2\pi\} \\ &= \sqrt{G_{P_{jj}}(\omega)} \end{aligned} \tag{2.11}$$

as $\delta\omega = 0.5\Delta\omega$.

In order to finally obtain the interior sound pressure level caused by the interface forces, the corresponding *Noise Transfer Function* (NTF) of the car is used. The NTF transfers the forces acting on the interface points to the final receiving point of interior sound pressure levels. In Figure 2.3, the whole procedure of the spindle load procedure is illustrated.

Figure 2.3: Overview of the spindle load measurement procedure.

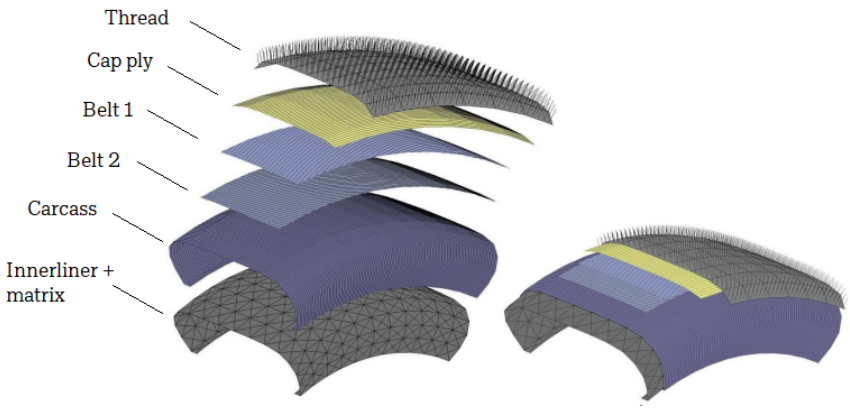

Figure 2.4: Illustration of CDTire/3D functional shell layer concept, ITWM [2022]

2.4 CDTire

CDTire is a semi-physical tire model family, designed to represent the functional performance of radial tires in complex multi body simulations, NVH- & linear-analyses for comfort and durability. The different models are adapted to balance accuracy and performance for different types of applications. It can be used to compute spindle forces and moments acting on each wheel as well as local contact forces during testing on a 3D road surface. Bäcker and Gallrein [2016].

2.4.1 CDTire/3D

CDTire/3D is a 3D shell based model that is built up using separate functional layer formulation. This results in separate representation of each component layer of the tire, for example inner liner, carcass, steel belt layers, cap plies & tread. The separated representation enables the model to be completely configurable. For example, the number of steel belt layers are arbitrary and associated belt angles together with the local material stiffness can be specific for each layer. Finally, the separate functional layers are condensed into one single shell representation. Gallrein et. al. [2018]. An illustration of the functional shell layer concept can be seen in Figure 2.4.

2.4.2 CDTire/NVH

CDTire/NVH is a software toolbox that derives a linear model from CDTire/3D for a pre loaded rolling tire. This model is the one that will be implemented in NVHD for analysis. CDTire/NVH is only compatible with NVHD version 2021.2 or newer due to software limitations. As version 2021.2 is the newest version available at VCC at the time of this thesis, it is restricted to use this version. When setting

up the environment, a parameter file that describes the physical properties of the tire is needed. CDTire offers a special tool for parameter identification, CDTire/PI, which bases on measurement data from the tire and assists in finding the optimal parameter set, ITWM [2022]. For the work presented in this thesis the parameter identification was performed by *Pirelli*.

In addition to the parameter file, the CDTire model also requires properties of the rim as well as the operating conditions. The operating conditions are expressed in terms of pressure, pre load, velocity, length and width of the contact patch and number of patch points in the direction of x and y, respectively. As advanced options, there are also possibilities to define the slip angle, inclination angle and drive torque. The operating temperature of the tire is not possible to change but is implicitly set by the temperature during the tire measurements in the parameterization.

The tire is loaded in the non-linear, transient generation phase, running on flat. During linearization, the patch point excitations are generated by systematically evaluating the steady state tire with a dedicated road surface model, utilizing both positive and negative z-variations according to Figure 2.5. Implementation in NVHD restricts CDTire/NVH to allow one single data line as input, used along the full width of the tire. This means that the patch points with equal distance in x are always being excited with the same amplitude at the same instance of time while there is a phase delay between points along the x-axis. The phase delay between two adjacent patch points corresponds to their relative distance Δx and the chosen analysis velocity v according to Equation 2.12. It should be noted that neither CDTire nor CDTire/NVH in general has this restriction. CDTire/NVH has the capability of independent input (in z-direction) for each single patch point.

$$t = \frac{\Delta x}{v} \tag{2.12}$$

Both ISO-B surface and scanned road surface can be used as input for patch point excitation, where scanned road surface is to be used in this project. How the road surface data is extracted is further explained in Section 2.5.

2.5 Scanned road surface

The road surface used in the physical measurements will be scanned in order to be used in the simulations. By 3D-scanning, the road surface data is stored in an open *Curved Regular Grid* (CRG) format where (CRG) is the specified file extension. This format was developed to describe road surfaces with high-precision, by storing elevation data from scanned surfaces. The format bases on the principle of placing data onto a grid along a reference line, OpenCRG [2022]. Each cell in the grid has a value, usually elevation which is the case for the current project.

From the stored CRG data, lines running along the travel path of the tire patches

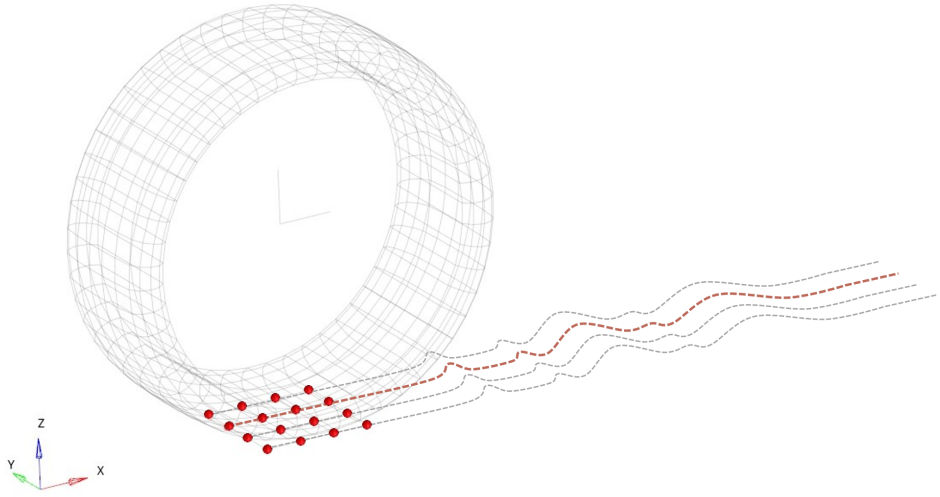

Figure 2.5: Patch points of a CDTire model.

can be extracted. The lines are extracted in *csv*-format, containing coordinates in x (travel path) and z (elevation) direction. The data can then be used as road profile input for the analysis setup in NVHD.

In the complete vehicle analysis setup using road surface data, NVHD allows three different alternatives when it comes to the number of input data lines. The first alternative is defined as single road profile which means that one road profile is used for all tires. The second alternative is based on two different road profiles, one for each side of the vehicle regardless of the front or rear tire. The third and last alternative is based on four unique road profiles, one for each tire.

2.6 Random response analysis with CDTire

The scanned road surface can be considered as a non-deterministic excitation. Due to the unpredictable roughness of the surface, it can neither be expressed by a harmonic nor a periodic function since it would involve too many dependent variables. Instead, the excitation can be described in terms of a statistical regularity where the statistical properties of the excitation are assumed to be constant independently of the chosen time origin. It is also assumed that a sample average for several different signals remain constant i.e. a stationary ergodic random process.

By using a *Fast Fourier Transform* (FFT), the extracted data line along the tire travel path can first be converted into frequency domain and further expressed as a *Power Spectral Density* (PSD) of the signal in spatial domain, Parmar et. al. [2020]. The PSD thus characterizing the energy content of the stationary random signal which can be used independently of the vehicle characteristics and velocity in simulations. In terms of the full vehicle model with one or several road profiles used in the simulations, there will be as many PSD signals as used profiles.

When using one or two road profiles in the analysis, the correlation between the front and the rear wheel could either be taken into account or not. In the same way as the phase delay in a single tire ensures that the different patch points being excited correctly according to the vehicle speed, a phase delay between the front and rear wheel could be applied as well. To account for the interaction between several PSD signals, a CSD matrix is calculated and used as the overall excitation input.

The full analysis is then based on two or more subcases, once again dependent on the chosen number of road profiles. The first case(s) corresponds to the sensitivity, or the FRF, of the vehicle when applying a unit displacement at each patch point with any associated phase delay. The last one corresponds to the random response analysis using the CSD as the excitation input.

Mathematically, this procedure have strong similarities with the spindle load method and the equations presented in Section 2.3. Independently of which type of correlation and how many road profiles that are used in the analysis, the response can be calculated according to Equation 2.13. $\mathbf{H_T}$ corresponds to the overall transfer function for all tire patch points at each wheel, including the corresponding phase delays, and $\mathbf{G_D}$ corresponds to the CSD-matrix of the overall excitation. If the front and rear tires are uncorrelated or correlated, the cross members of the CSD-matrix are either all- or non- zero respectively. $\mathbf{S_X}$ corresponds to the PSD of the response, either explained in terms of displacement, velocity, acceleration or pressure.

$$\mathbf{S_X} = \mathbf{H_T G_D H_T^{+H}} \tag{2.13}$$

3

Measurement-based predictions and validation data

This chapter presents how the interior noise measurement was performed as well as the spindle load method. The general setup for the physical testing is presented, including specification of used vehicle, tires and road data. The data collected will be compared against the simulation-based predictions presented in Chapter 4.

3.1 General set up

The car used is as previously mentioned in Section 1.4 a Volvo XC90 production car with an internal combustion engine and the set of tires used are *Pirelli PZERO 275/35 R22* without (PNCS). These tires are normally equipped with a cavity foam PNCS inside them which reduces cavity noise, however for these measurements the cavity foam was never installed. Reason why is ensuring that cavity peaks occur, enabling an evaluation of the predictive capability of the CDTire/NVH model. Two different tire pressures were measured, 2.4 & 2.8 bar.

The measurement was conducted at Volvo Hällered proving ground on Barfield road. Barfield is referred to as a country road where impacts occur along the travel path which generates a varied excitation. The test was conducted at 50 km/h which is the velocity that is valid for evaluation against VCC's requirements. To ensure a constant and correct vehicle speed, a calibrated GPS device was used during the measurements.

There are certain requirements set by VCC that needs to be fulfilled when performing measurements. The road surface needs to be dry and the ambient temperature should be above 5°C in order to be able to warm up the tires enough. Tires are warmed up until the tire temperature have reached steady state with respect to speed and ambient temperature before performing the measurements. VCC measurement protocol requires the temperature to be at least 30°C. This is achieved by driving on a high-speed track and measuring the average temperature of the grooves in the tire tread using a thermal imager. Figure 3.1 displays a thermal imager aimed at a warmed up tire, measuring the temperature in one of the grooves.

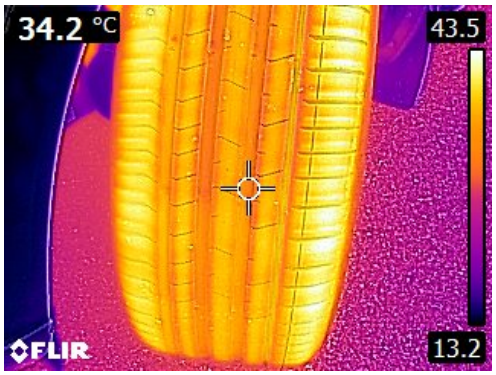

Figure 3.1: Thermal image of heated tire.

(a) Mounted interior mics.

(b) Overview of interior microphones placement.

Figure 3.2: Interior mic placement

3.2 Interior noise measurements

The interior noise was measured using 6 microphones mounted in the interior of the car. The mics were mounted at positions that represent the driver's & front seat passenger's outer and inner ear respectively and the rear seat passengers' outer ears. Figures 3.2a & 3.2b illustrate how the mics were mounted and an overview of the positioning of the mics in the car.

The mics were connected to a *Müller-BBM PAK*-measurement system that reads & transforms an analog input into a digital output. With the NVH software suite *PAK6* on a computer connected to the measurement system, all channels could be visualized and observed whether an overload occurred during the measurements. Each interior mic was represented by a separate channel.

After an initial check that a signal was received from all channels, runs on the track were measured until one successful measurement was collected. The raw data obtained by the measurements contains sound pressures in the time domain for all

interior mics. Post processing was done in MetaPost where interior noise for all mics were plotted and evaluated.

3.3 Spindle load method

The implementation of spindle load measurements was divided into three steps, measuring accelerations, computing spindle loads and interior noise. The requirements for the analysis was a complete vehicle FE-model along with trimmed body NTF:s and vibration transfer functions from interface points. All accelerometer and microphone data were collected in the same recording, to ensure correct phase data.

3.3.1 Accelerometer measurements

First step before measuring the accelerations is mounting accelerometers on the knuckles, five accelerometers on each knuckle resulting in 20 in total. Five accelerometers per knuckle is in fact not needed however it makes the system overdetermined, reducing measurement errors.

The accelerometers were mounted on spacers which then were glued on the knuckles at different positions. Each accelerometer has its own local coordinate system which needed to be aligned with the global coordinate system of the complete vehicle. Due to this, mounting needed to be precise in order to get correct alignment and to prevent misleading directional contributions.

In Figure 3.3a a closeup of a mounted accelerometer is presented. Figure 3.3b displays the positioning and numbering of all accelerometers mounted on the front left knuckle. The mounting setup on the front right knuckle were equal but mirrored, while the mounting on the rear knuckles were different as they differs in shape. However, the mounting positions were similar for these knuckles.

(a) Accelerometer 193.

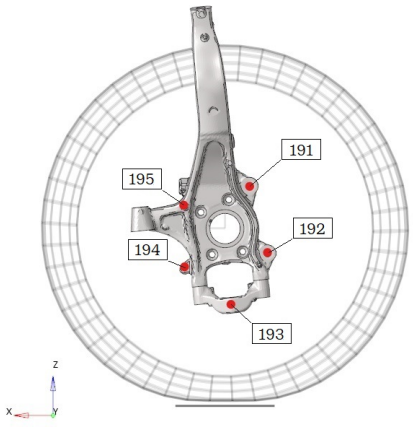

(b) Mounting positions on front left knuckle.

Figure 3.3: Accelerometer mounting.

All accelerometers were connected by cables which were drawn from each knuckle through the rear doors into the interior of the car. The cabling was connected to the *PAK*-measurement system described earlier in Section 3.2 where just as for the interior mics, all accelerometers had individual channels for visualization and observation in the *PAK6* software suite. The collected data was stored on *unv*-format, containing accelerations in x-, y- & z-directions in the time domain. This data was then used as input in the next step, computing spindle loads.

3.3.2 Spindle load

To compute spindle loads, VCC has created a GUI & scripts in *Matlab* to simplify the process. The GUI consists of five steps, starting from measured accelerations on the knuckles to the final output of the CSD-matrix $\mathbf{G_F}$ at the wheel center.

First step is to convert the measured time-data from *unv*-format to *mat*-format. Secondly the spindle FRF:s $\mathbf{H_s}$ that are obtained in *pch*-format from NVHD are converted to *mat*-format as well. After that, $\mathbf{H_s}$ is sorted in order to obtain correct numbering of nodes for compatibility with measurement data.

Next step is to create the CSD-matrix $\mathbf{G_a}$. This step in the GUI makes a FFT of the time-data and uses Welch's method to compare the $\mathbf{G_a}$-matrix. The GUI offers option of selecting between full CSD of $\mathbf{G_a}$-matrix, partly or no cross PSD where the last one removes cross-spectrum of the wheels. With $\mathbf{H_s}$ and $\mathbf{G_a}$ obtained, the final step is to compute the spindle force CSD $\mathbf{G_F}$. With $\mathbf{G_F}$ obtained, the GUI process is complete and the next step is to combine the spindle loads with the chassis FRF:s $\mathbf{H_v}$. To obtain the forces at the interface points between chassis and body, the procedure that were described in the latter part of Section 2.3 is used.

3.3.3 Interior noise

In order to transfer the spindle loads into interior noise and make accurate comparisons to known data and requirements, VCC has developed an automated shell script procedure. The procedure itself is divided into four parts, where calculations and processing of data are executed using *Python* scripts, *MetaPost* and *Optistruct*.

The previously obtained interface forces are, together with NTF and additional required model information, defined in a script created for the procedure. The script takes the chassis input deck in *fem*-format as input and gives chassis FRF on *pch*-format and a $\mathbf{G_p}$ force file as output.

Additional output from the script is MetaPost script files for plots of interior noise, interface points force, TPA, spindle TPA and averaged quadratic sound pressure. RMS values and TPA for the different frequency regions are also obtained. The defined frequency regions are rumble, cavity and rough tire noise whose ranges are set in the user input settings for the script. TPA will be performed at three frequency peaks, one in the rumble range (60-160Hz) and two in the cavity range (160-220Hz).

4

Simulation-based predictions

This chapter treats the simulation-based predictions using same general setup presented as in Section 3.1. Initially a single tire validation of the CDTire/NVH model is presented, followed by how the scanned road surface data was processed & extracted. However, this chapter mainly presents the setup and analysis of the complete vehicle simulation including CDTire/NVH tire models in NVH Director.

4.1 Single tire validation

Before setting up a complete vehicle analysis, single tire simulations were performed in order to validate the tire model and investigate its characteristics.

A rigid point was created and used to constrain the tire in all directions except rotation around the y-axis which enabled rotation in the travel direction. The tire module was created in NVHD using the CDTire/NVH software toolbox. A parameter file was provided by *Pirelli* and additional wheel parameters were provided by VCC which are listed in Table 4.1. The operating temperature were estimated from the parameter file to be approximately 20°C.

As can be observed in Table 4.1, the pre loading differs between the front & rear tires and the camber angles are separate for each tire. This means that the complete vehicle simulations requires four separate CDTire/NVH models in order to repre-

Table 4.1: Wheel parameters

Wheel parameters	
Rim inertia [x,y,z]	[0.589, 0.941, 0.59] kgm^2
Rim mass	18.5 kg
Patchpoints [x,y]	[8,8]
Tire pressure	(2.4, 2.8) bar
Pre load front	5680 N
Pre load rear	5528 N
Inclination angle front [Left/Right]	$[-0.9°/+0.9°]$
Inclination angle rear [Left/Right]	$[-0.9°/+0.9°]$

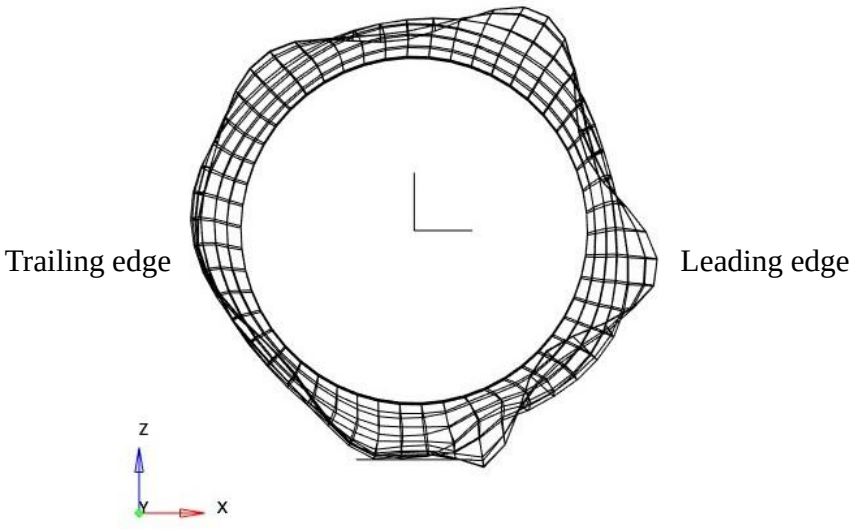

Figure 4.1: A single tire excited by a shaker at 185Hz.

sent the characteristics correctly. However, only one tire was initially analyzed for validation with the operating velocity set to positive 50km/h.

Both the number of patch points and the dimensions of the patch area in both x- & y-direction were defined by recommendations from *Altair*. The number of patch points were set to eight in both directions, resulting in 64 patch points in total. The required dimensions of the patch area depends on the actual tire used in the analysis. An important parameter is the width of the patch area, which must be as wide or even wider than the actual tire to ensure correct excitation at all patch points. Since the *Pirelli* tire is 0.275m, the patch area was defined as 0.2×0.3m in x and y respectively. Using a narrower patch width than the tire itself has shown to be problematic and may cause unrealistic excitation at some patch points.

The analysis type was set to shaker excitation, which is a predefined load case by VCC that kinematically excites all patch points uniformly in the interval of 10-400 Hz. The excitation is an enforced displacement in positive z-direction that in turn generates forces on the wheel centre. The tire parameters were set according to a front left tire, namely a negative camber angle of 0.9° and corresponding pre load for a front tire with a velocity of 50km/h. Normally a negative camber angle is associated with a positive inclination angle for the front left tire. However, CDTire/NVH is using a coordinate system with x-axis pointing forward and therefore the front left tire has a negative inclination angle.

The completed simulation was analyzed in NVHD. Figure 4.1 displays a tire with an implemented CDTire-model where the Doppler shift effect, discussed in Subsection 2.1.1, can be observed. The shorter wavelengths can be observed on the leading edge of the tire while the waves on the trailing edge appears to be longer. According to the Doppler shift effect this means that the rotational direction of the tire corresponds to a positive x-direction.

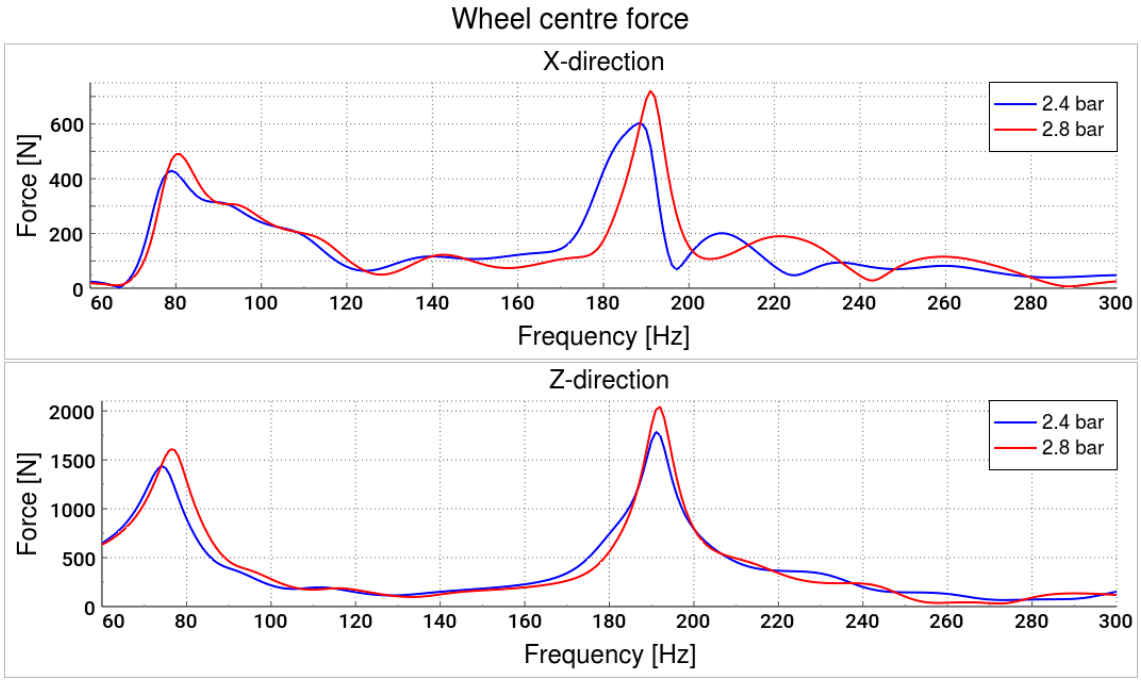

Figure 4.2: Wheel centre force in x & z-direction for two different tire pressures, excited by a shaker at 50km/h.

By looking at the wheel centre forces in x & z-direction where the cavity peaks normally occur, presented in Figure 4.2, it seems like the expected cavity split is not clearly visible. For a tire with dimensions according to Section 3.1, a velocity of 50km/h and a temperature of 35°C, the cavity peaks can be expected from Equation 2.1 to appear at around 175Hz and 187Hz. However, only the peak of the higher resonance frequency seems to appear in both directions. It is possible that the simplified road excitation is augmenting the response of the tire and is therefore the cause of this unexpected tire response. In order to further investigate the behaviour, different combinations of pre load and velocities were tested and will be presented in Section 5.1.

4.2 Scanned road surface

The scanned road surface data in OpenCRG-files was post-processed in *Matlab* as OpenCRG [2022] includes a software library for Matlab that enables modifying, creating and visualizing this type of data. The tool suite includes both scripts for processing and plotting CRG-files but also demo data to assist in learning how to use the tools. Initially the demo data was used to get familiar with the environment but also to write an own script to extract lines along the travel path for use in NVHD.

User settings for the script define coordinates of the tires when the data should start being extracted and how many meters it should extract. As CDTire/NVH in NVHD is only capable of reading in a single value of data across the width, the front

and rear tire for each side would receive nearly same excitation as the tire paths are strictly similar. Due to this, two road profile was chosen and thereby two unique lines were extracted.

An example of a road surface and the lines being extracted is visualized in figure Figure 4.3. The road data being used is from the provided demo-data by the tool suite. The extracted lines represent the LHS & RHS tires of the car which then were used as input when setting up a model analysis in NVHD.

The number of data points for the whole Barfield road is too large to easily visualize its road surface similar to the demo data. Instead Figure 4.4 displays the elevation for one extracted data line along the travel path. The figure also includes a zoom-in of the data for a more detailed view of how the surface varies along 0.5m with its resolution of 5mm. The road starts on $x = 671$m due to a global coordinate system from the scanned road data that covers additional area.

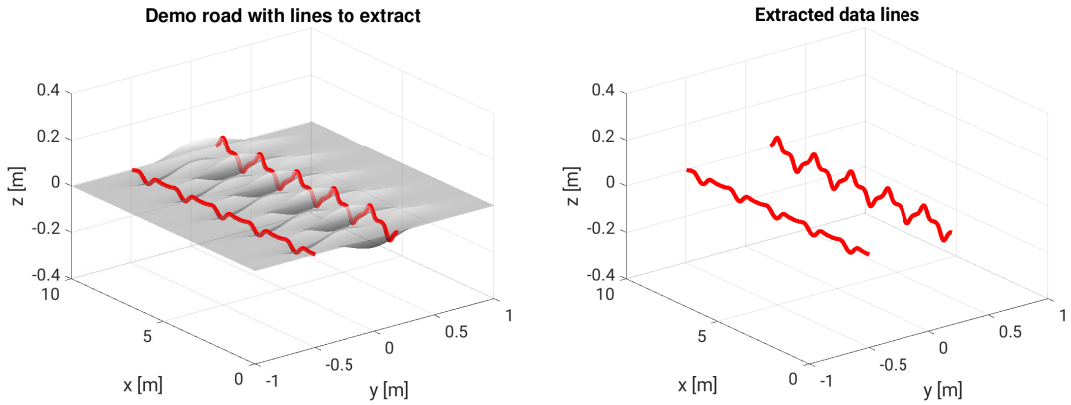

(a) **(b)**

Figure 4.3: Demo road surface and example lines for extraction.

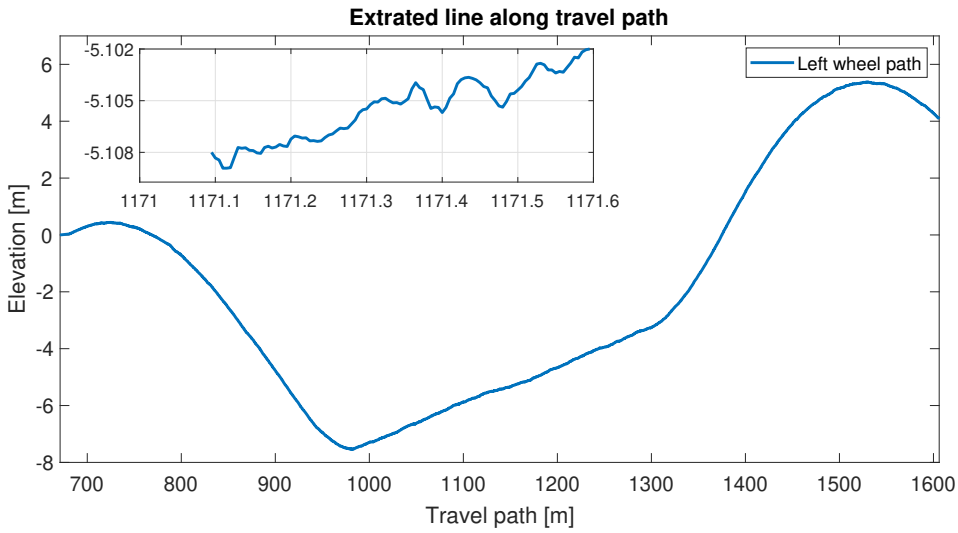

Figure 4.4: Elevation of the Barfield road along the travel path with a magnification at 1171m.

4.3 Complete vehicle simulation

After completing the single tire validation, confirming model characteristics and parameter settings, the complete vehicle model was set up and analyzed. A full FE-model of the car with an included cabin cavity model was provided by VCC. The model is defined such that its forward vehicle cabin direction is in the negative x-direction in the coordinate system.

4.3.1 Model setup and validation

First step was removing previous tire modules from the model, insert and re-position the new CDTire modules. As the tire modules are defined in a positive, hence opposite x-direction relatively to the vehicle model, the velocities of the tires were set with a negative sign. As of now the coordinate systems of the tires cannot be chosen but is something that is currently being implemented by *Altair*. In order to observe the behavior of the tires when they were positioned and connected to the full vehicle, the shaker excitation analysis was initially set up. For the full vehicle model, the shaker excitation case corresponds to a uniform excitation of all four tires and their associated patch points without any phase delay. According to Figure 4.5, the waves of the tires corresponds to a forward pointing direction of the car which is the desired behaviour for the analyses. Thereby it can be concluded that a negative velocity in the tire modules ensures correct rotational direction of the tires, hence the correct gyroscopic effects.

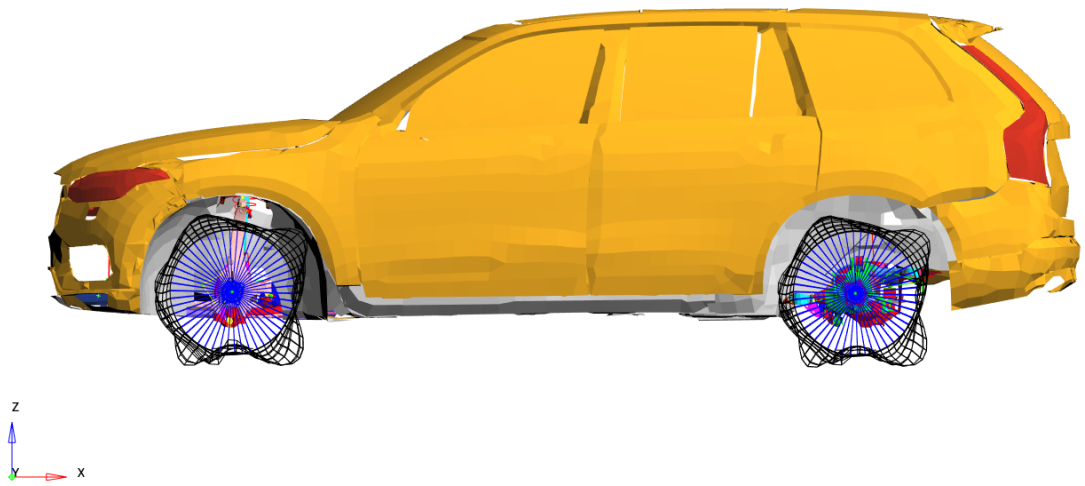

Figure 4.5: Shaker excitation on complete vehicle model.

4.3.2 Model analysis

After running shaker excitation analyses and confirming correct rotations and behaviours of the tires, a road profile analysis was set up. The input data was collected & extracted as described in Section 4.2. Corresponding PSD data of the road excitation was calculated and also exported for later use in post processing. The vehicle velocity was defined with a positive sign as the loadcase setup by default is defined accordingly to the car's forward pointing direction. This results in a negative velocity obliged to be defined for the tire modules and a positive velocity in the analysis setup which is currently being revised by *Altair*. Front to rear tire correlation was enabled and calculated in order to get the correct phase delay between the front and rear tires.

Next step in the analysis setup was the diagnostic setup. The selected response points were the interior mics, the interface points between chassis and body and the points where all accelerometers were mounted in the measurements. By selecting not only the interior mics as response points, but other response points along the transfer path as well, made it possible to divide the comparison into three steps. This made it easier to understand the behaviour of the complete vehicle model and not only the interior noise caused by the tire patch excitation. With the loadcase and analysis setup completed, the settings were applied and corresponding *fem*-file was obtained for job submission.

4.3.3 Transfer path analyses

In addition to above described settings for the analysis setup, Auto TPA was also enabled. The car's body was defined as the control volume and earlier defined

response points were selected. Since TPA analyses in NVHD for random responses is only possible at a specific frequency at a time, represented as a bar plot, it is important to either solve the Auto TPA for the full interval or by selecting desired frequencies. The latter alternative reduce the computational time but requires on the other hand that the frequencies of interest are already known.

4.3.4 Post-processing

As a final step in the complete vehicle simulation, the resulting data from the analyses was post-processed in Hyperview and MetaPost. In Hyperview, the NVH integrated diagnostic tool was used to visualize the TPA analyses by importing the FRF of the complete vehicle and the exported forces from the road excitation. The five interface points with highest contribution to the sensitivity were represented in a bar plot, where the contribution could be either positive or negative to the sensitivity. Positive and negative contributions corresponds to an in- or out-of-phase amplitude respectively, relative to the sensitivity of the vehicle.

The resulting data at chosen response points was processed and plotted in MetaPost which enabled alternatives for weighting, filtering and plotting the curves in order to make comparisons as viewable as possible. All results are presented in Chapter 5.

5

Results

The following chapter presents the results of what all simulations and measurements have culminated in. Overall comments and conclusions for each result are also presented in each section while more in-depth analysis will be discussed in Chapter 6. Henceforth, the complete CDTire analysis described in Chapter 4 will only be referred as CDTire.

5.1 Single tire evaluation

As the cavity peaks that were expected for the single tire simulation did not appear, further investigation of what may have caused this was performed. Different parameters such as velocity and pre load were halved and doubled separately in order to evaluate whether these had any influence on the unexpected behaviour. Figure 5.1 displays a comparison in both x- & z-direction with different configurations of velocity and pre load with a tire pressure of 2.4bar. Since the behaviour for both 2.4 and 2.8bar were similar with respect to the peaks, only a tire with 2.4bar were tested further.

Independently of the pre load at 50km/h, there is no clear split of the cavity peaks, only one wider peak occur at around $185 - 190$Hz. In the case of 25km/h, there is a clear split for both pre loads in the x-direction, however they differ from the theoretically values at around 178Hz and 184Hz from Equation 2.1. For the vehicle speed of 100km/h, the cavity mode split is clearly visible for the pre load of 5680N but significantly less for the higher pre load of 11360N. The corresponding theoretically values at 100km/h occur at around 169Hz and 193Hz. As mentioned already in 4.1, only the peak of the higher resonance frequency appears in the frequency response of the wheel center forces which might be possibly due to the simplified road excitation.

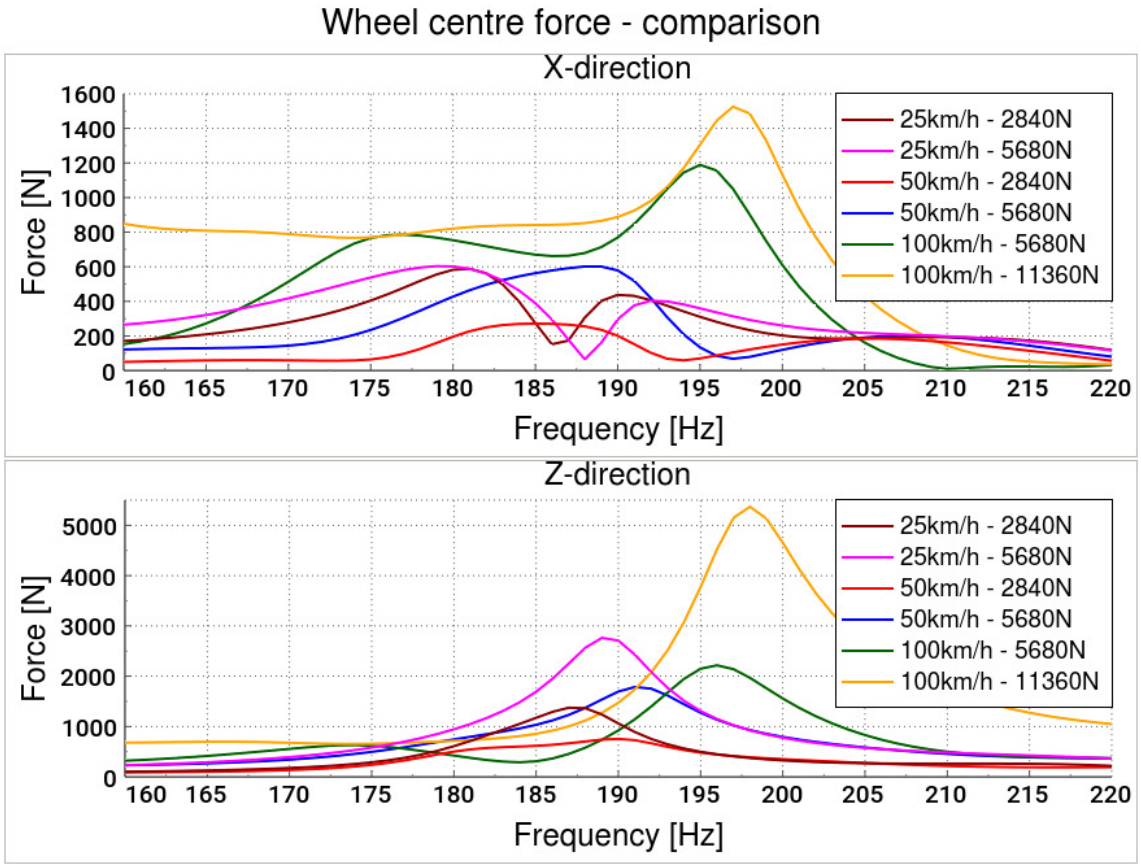

Figure 5.1: Wheel centre forces in x & z-direction for varying load conditions.

5.2 Accelerometer response

When conducting the measurements, 20 accelerometers in total were used for all knuckles. Results from two of the accelerometers, 294 & 392, are presented along with corresponding simulation results using the CDTire model. Accelerometer 294 is presented in Figure 5.2 and Figure 5.3 while results for 392 can be observed in Appendix A. Only two accelerometers, one for the front and rear tires respectively, are presented as they all demonstrate similar results regarding the predictability of the CDTire model. Accelerometer 294 belong to the front right tire and 392 to the rear left tire. Accelerations in x-, y- & z-direction are presented in the frequency range 60-300Hz and are weighted using a dB(A) filter.

Figure 5.2 presents accelerations measured on accelerometer 294 with tire pressure 2.4 bar followed by Figure 5.3 that displays the same measurement but with a tire pressure of 2.8 bar. A corresponding comparison at accelerometer position 392 is presented in Figure A.1 & Figure A.2 in Appendix A.

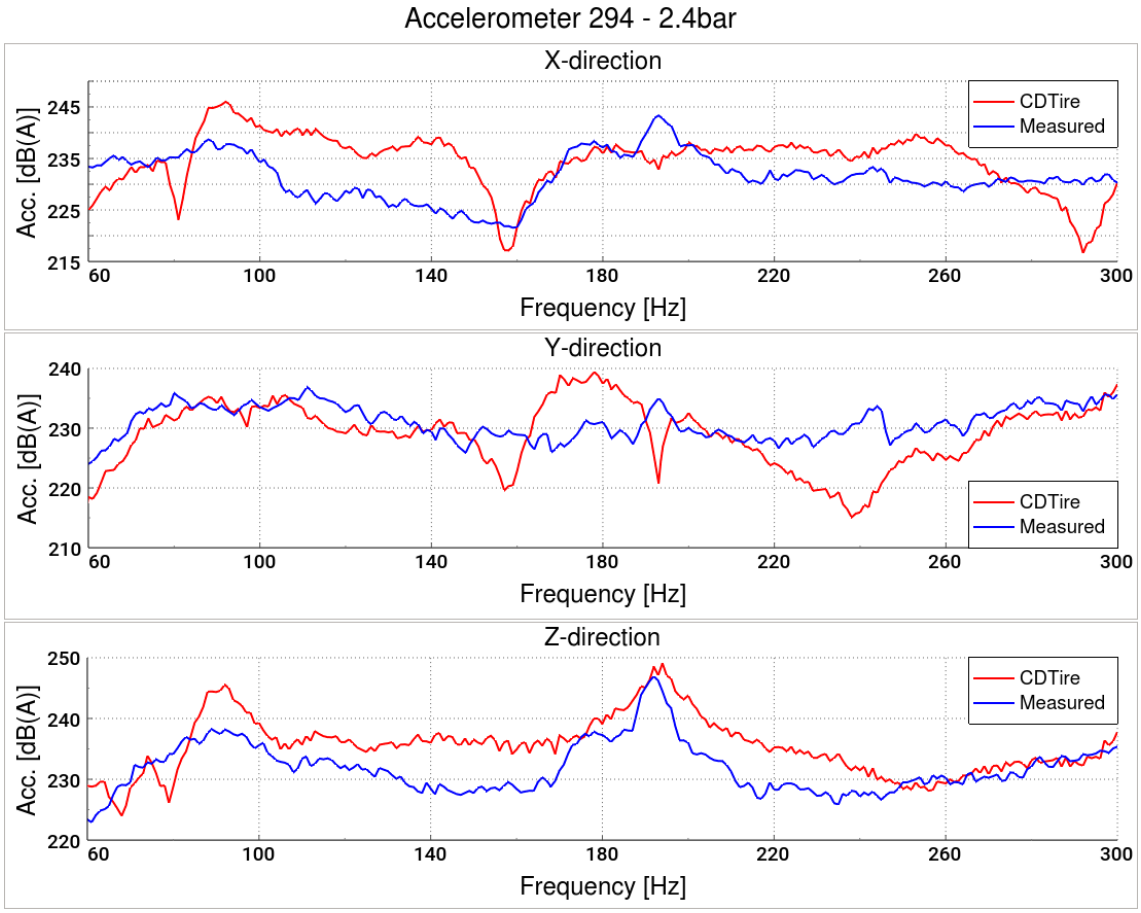

Figure 5.2: Acceleration response at position 294 from measurements and CDTire analysis for 2.4bar.

The response in Figure 5.2 show that the measured data in x-direction capture the expected cavity peaks at around 175Hz and 187Hz, while CDTire/NVH does not show any clear peaks. In y-direction, there are no clear peaks in either the measurement data or from CDTire/NVH while the higher peak occur clearly in z-direction. However, the higher resonance frequency is predicted at a slightly higher frequency than what the measurement shows.

For the responses with a tire pressure of 2.8bar in Figure 5.3, the measurement show two cavity peaks in z-direction at expected frequencies while CDTire does not show any clear cavity peaks. A tendency to a peak may be seen at 180Hz in x- & z-direction for CDTire/NVH, however it is significantly less distinct compared to the measurement. These results in combination with the ones obtained for 2.4bar tire pressure indicates a non-robustness with CDTire/NVH in NVHD's ability to capture cavity modes correctly.

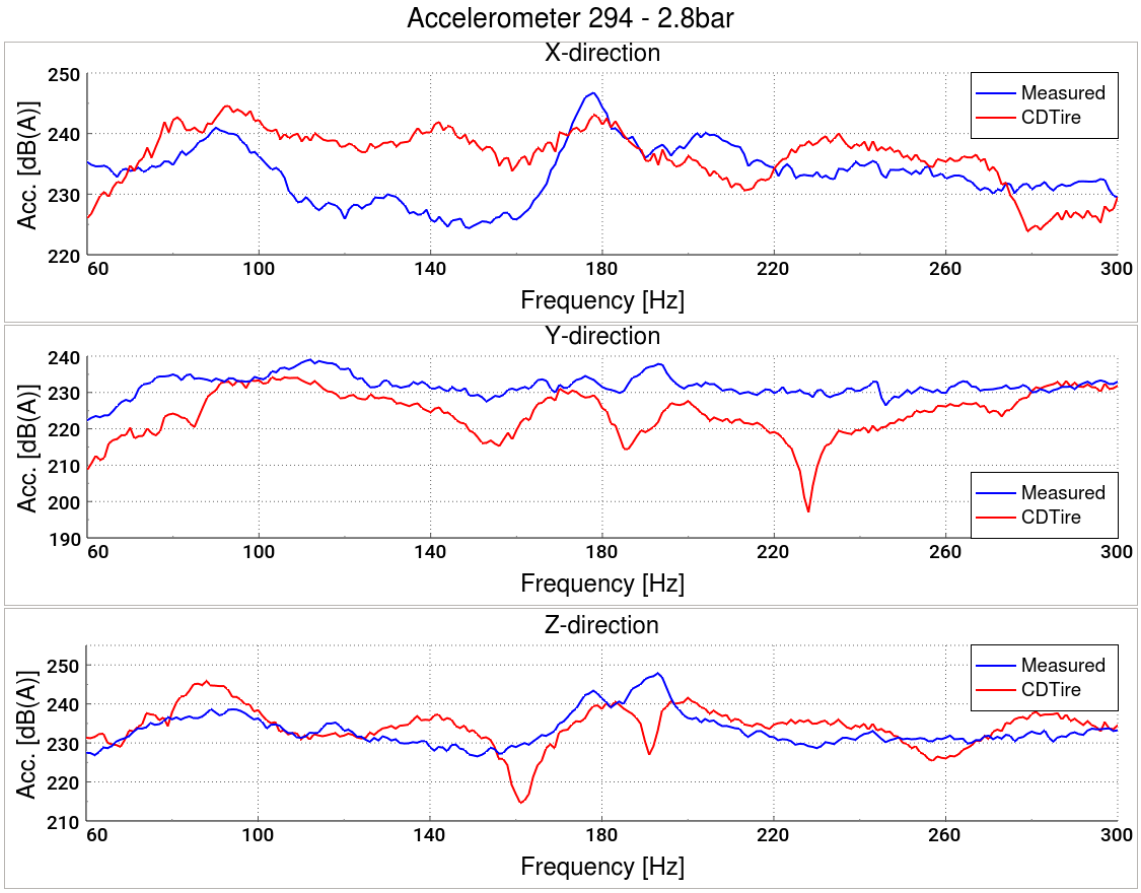

Figure 5.3: Acceleration response at position 294 from measurements and CDTire analysis for 2.8bar.

5.3 Interface forces

Forces in the interface points between chassis and body were outputs from both the spindle load method and CDTire simulations for a tire with 2.4 bar. The forces at the points were obtained in both x-, y- & z- direction however only z-direction is presented in Figure 5.4. The interface force on the vertical axis is weighted with dB(A) relative to 1N.

The predicted forces from the spindle load method show a decreasing behavior for higher frequencies while the forces from CDTire show a slightly upward going trend instead. The cavity peak at around 187Hz is only captured by the spindle load method and not by CDTire predictions. While the response from the spindle load method is quite stable, the CDTire show a unexpected significant ripple which indicates that there is something wrong in the predictions which will be further discussed in Section 6.3.

Figure 5.4: Interface force in z-direction at point 101 from spindle load method and CDTire analysis.

5.4 Interior noise

The resulting interior noise using the different methods and measurements for two tire pressures are presented in Figure 5.5 and Figure 5.6. Results from CDTire are displayed in two different curves, one with actual values and one with a centered moving average of 4 terms. The moving average is displayed to enable easier estimation and comparison since the unfiltered results from CDTire shows a strongly oscillating behaviour. The vertical axis is *Sound Pressure Level* (SPL) which is weighted using dB(A) filter relative to $2 \cdot 10^{-5}$Pa.

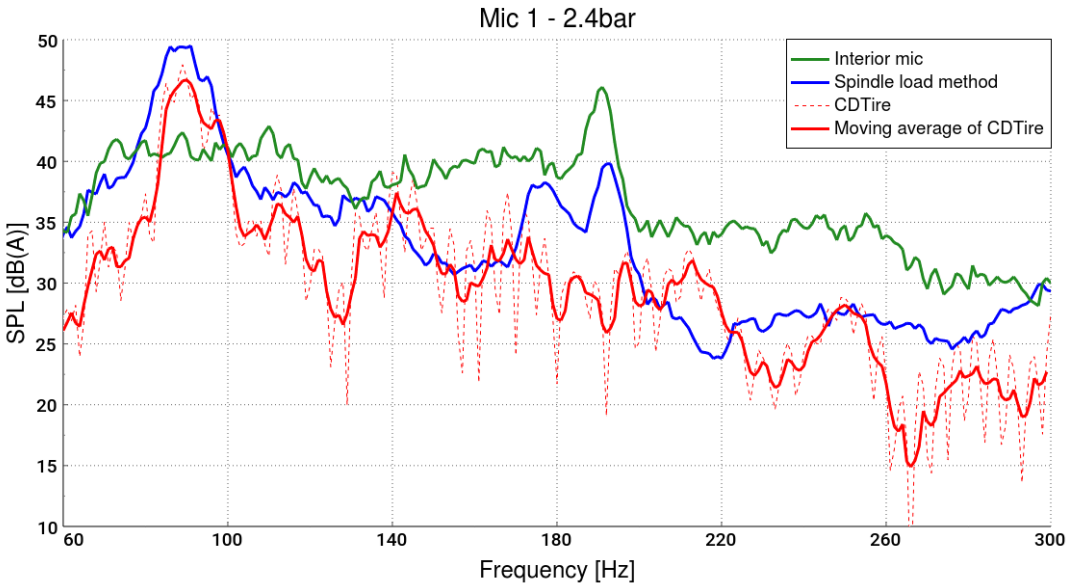

Figure 5.5: Interior noise level at mic 1 for 2.4 bar.

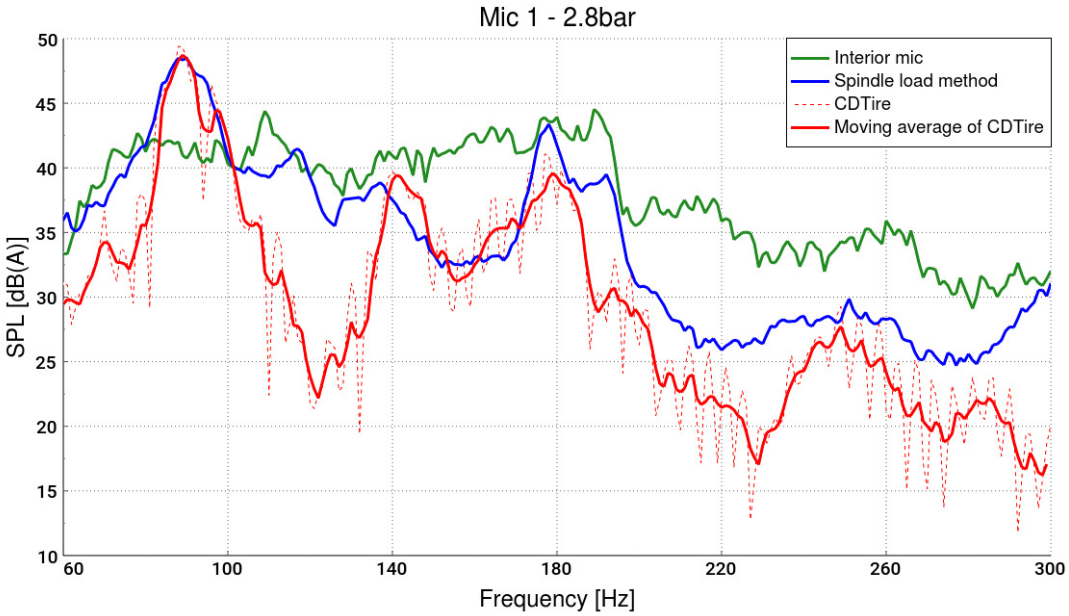

Figure 5.6: Interior noise level at mic 1 for 2.8 bar.

Resulting interior noise for both tire pressures show that CDTire is able to capture the peak occurring in the rumble range around 90Hz. However, CDTire otherwise appears to underpredict SPL in comparison to measurement & the spindle load method. In Figure 5.5 CDTire is not able to capture the higher cavity peak around 190Hz that is clearly captured by measurement & spindle load method. In Figure 5.6 CDTire seems to capture the first cavity peak however the absolute value differs in comparison with the other two curves. In general CDTire appears to experience significantly more fluctuations in absolute values which implies sensitivity & robustness issues with the model.

5.4.1 Varying pre load

As a further investigation of how the tire pre load affects the response, a full analysis of the interior noise was performed using tires where the pre loads were halved according to Table 4.1. The responses are presented in Figure 5.7 where the curves for the spindle load method and CDTire - 5680N are the same as in Figure 5.5 and are included for comparison.

With a halved pre load, CDTire seems to capture the first cavity peak clearly but obtains a remarkably larger amplitude compared to default pre load and spindle load method. The difference in interior noise for the two different pre loads with CDTire is at 180Hz as high as 15dB which is an unreasonable increase. Clearly, the model is highly sensitive to pre load as the two curves distinguishes remarkably in absolute values and trends.

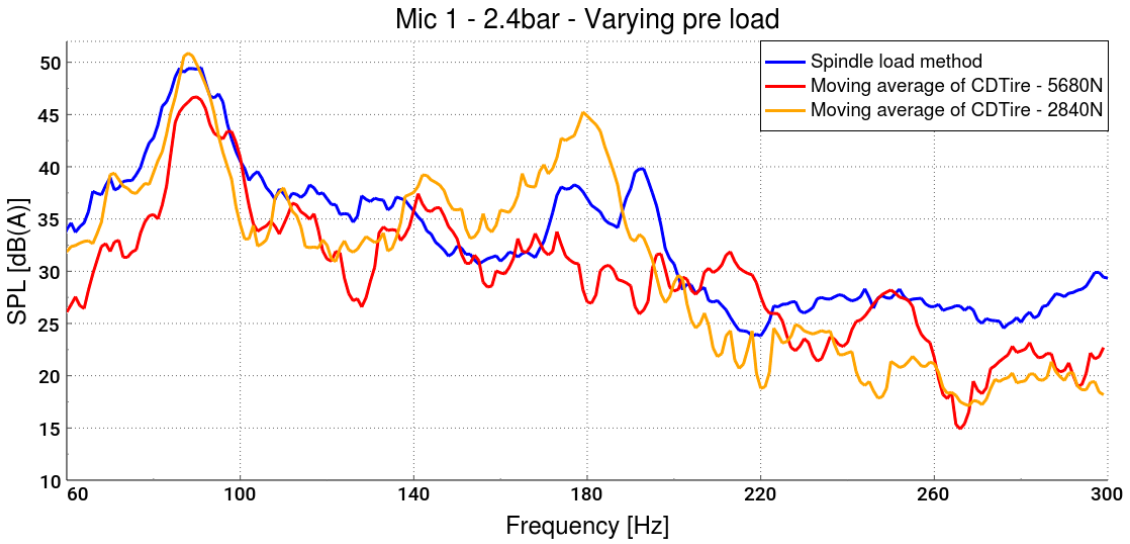

Figure 5.7: Interior noise level at mic 1 for 2.4 bar with a varying pre load of the CDTire model.

5.5 Delta study

Results from performed delta study is presented in figure Figure 5.8 which displays differences depending on tire pressure for both interior mic measurements, the spindle load method and by using CDTire. As obtained results with the CDTire model had oscillating behaviour, a moving average is displayed for easier evaluation of sound pressure levels.

Apart from the absolute difference between the two curves in the measured interior noise and the predicted values by the spindle load method, they show a consistent trend which the predictions from CDTire does not. In the first two cases, the response for 2.8bar tends to be of an equal or higher amplitude than for 2.4bar, which the predictions from CDTire does not show.

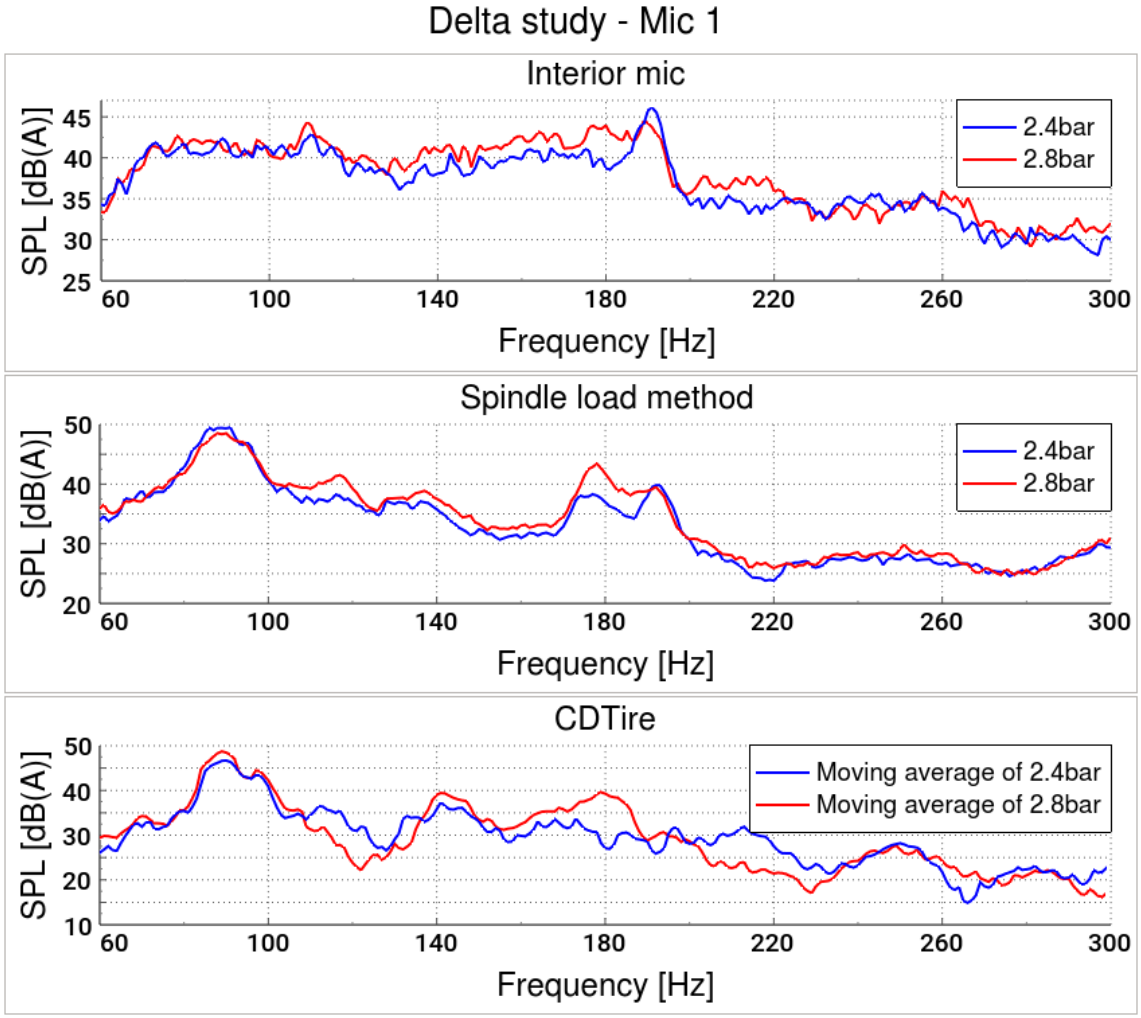

Figure 5.8: Delta study of the predicted sound pressure level for varying tire pressure.

5.6 TPA analyses

Figure 5.9 - 5.13 presents TPA analyses for a tire pressure of 2.4bar at three different frequencies, 90 Hz in the rumble range and 178 Hz & 191 Hz in the cavity range. Results from the spindle load method are presented with line graphs for the full frequency interval while CDTire results are presented with bar plots due to different post processing compatibility. The bar labels displayed in the CDTire results are all ending with either *T1*, *T2* or *T3* which corresponds to x-, y- & z-directions respectively. The legends in the line graphs in Figure 5.9 and Figure 5.11 lists the contributions in descending order. The corresponding comparisons between the spindle load method and the CDTire analyses for a tire pressure of 2.8bar is presented Appendix B.

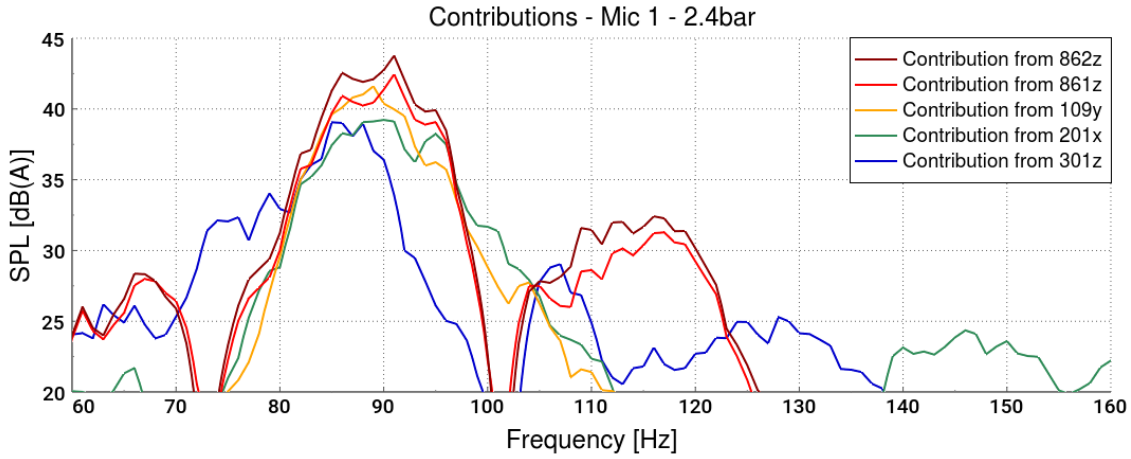

Figure 5.9: Top five contributors in the rumble interval predicted by the spindle load method at 2.4bar.

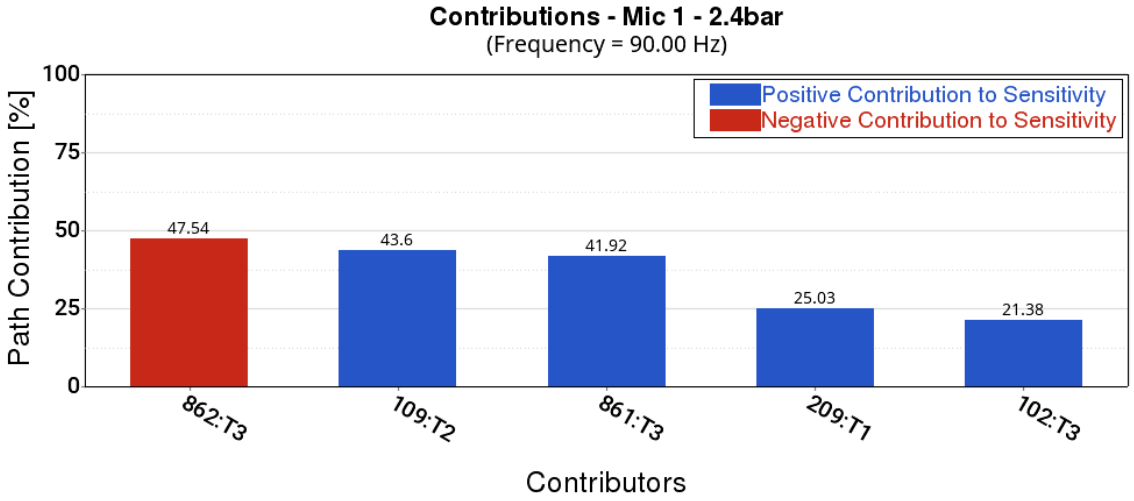

Figure 5.10: Top five contributors at the rumble peak predicted by CDTire at 2.4bar.

For the rumble peak at 90Hz presented in Figure 5.9 & Figure 5.10, CDTire predicts the same top three contributors as spindle load method which is considered to be a quite good prediction.

In the cavity range, presented by Figure 5.11-5.13, CDTire does not have same top contributor as for spindle load method. For both peaks only two contributors in the top five are included for both methods and both of them are ranked differently. However, previous shown results proved that CDTire struggles with capturing cavity peaks which consequently affects the TPA to be less pertinent. Hence, TPA may not be valid to use for analysis of contributions to the cavity peaks as long as the cavity peaks are not captured correctly.

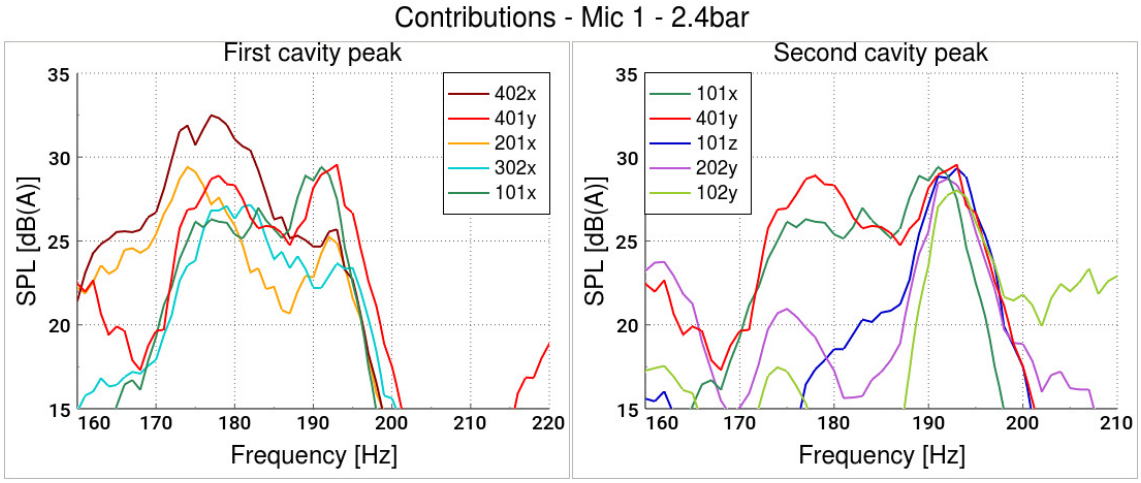

Figure 5.11: Top five contributors in the cavity interval predicted by the spindle load method at 2.4bar.

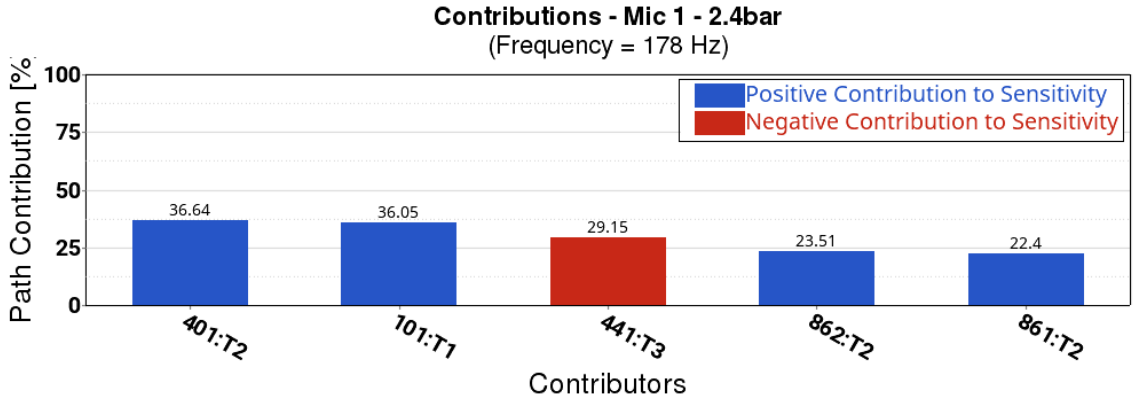

Figure 5.12: Top five contributors at the first cavity peak predicted by CDTire at 2.4bar.

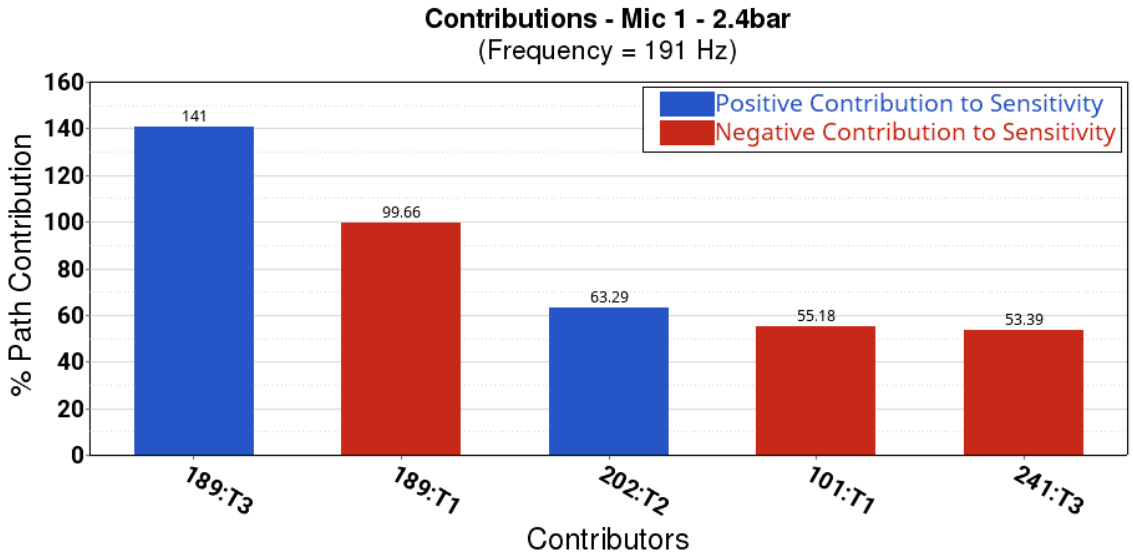

Figure 5.13: Top five contributors at the second cavity peak predicted by CDTire at 2.4bar.

6

Discussion

Obtained results are analyzed in the following chapter where a discussion is conducted on factors that may have affected the outcome and possible conclusions that can be drawn.

6.1 Physical measurements

Conducting physical measurements includes numerous factors that may affect the accuracy of the results. A key factor when conducting the measurements is the mounting of the accelerometers. If the accelerometers are not mounted exactly parallel against the global coordinate system, the component directions will be slightly offset and cause some of the excitation to wrongly shift in what component direction it acts.

Ensuring consistent tire temperature is also an uncertainty as it can only be noted in between the measurements. In addition, loose gravel occurs on the track which can cause unexpected impacts, overloading or harming the accelerometers. However, this is controlled when conducting the measurements as all channels are checked to ensure that no overload occurred.

6.2 Single Tire evaluation

From the results in Section 4.1, it seems like the combination of pre load and velocity have a strong influence on the response. However judging by the results, it is not that easy to draw conclusions on how the parameters are correlated against each other. For velocities at 50km/h, the pre load seems to have low influence on the peaks and only results in a varying amplitude of the curve. When the velocity is halved instead, two peaks occur independently of the pre load. As mentioned in Section 5.1, the theoretical values at 25km/h is not in total agreement with the results from the analysis. Even if the distance between the peaks and their location differs from the calculated ones, it still seems to be a reasonable cavity response.

In similarity to the case at 25km/h, the peaks at 100km/h from the analysis seems to appear higher in the frequency range than what the theoretical values does. Since

the equations in Subsection 2.1.1 does not take the pre load and its influence into account, it is however difficult to strictly compare the values. Even though the exact pre load is unknown, the response should not be significantly affected as it is only a geometric deformation of the tire. A halved or doubled pre load may shift the cavity peaks a few steps in the frequency band but not completely distort the locations of the peaks as if the tire would have been completely deformed.

By comparing the response at 25km/h and 100km/h, the cavity model anyway seems to act properly with respect to the Doppler shift effect. From the varying velocities, one should expect the split to be wider as the velocity increase, which is also the case. Why these peaks does not occur at 50km/h is a question that remains to be answered.

6.3 Responses

The accelerometer responses presented in Section 5.2 shows that CDTire/NVH in NVHD is able to predict similar absolute values compared to the spindle load method. There are differences but the predictions passes each other in magnitude and from this it cannot be concluded that CDTire/NVH would over- or under-predict responses on the accelerometers. However, CDTire/NVH in NVHD is not capturing the cavity peaks aligned with measurements. Either none or just one cavity peaks is captured and the peaks are not as distinguishing as for the measurements. Furthermore, interesting to remark upon is the behaviour of the CDTire/NVH in NVHD curve. While the spindle load curve is quite uniform aside from the up-pointing peaks in rumble & cavity range, CDTire/NVH in NVHD shows a more fluctuating behaviour with several downward peaking drops in magnitude. These fluctuations and drops in magnitude implies a sensitivity with the model.

From the results presented in Section 5.3, it is clear that the correlation between the methods is weak and the results from CDTire/NVH in NVHD shows strongly oscillating behaviour that is difficult to interpret. Interesting to note is that this behavior strongly differs from the accelerometer response where the response shows quite steady results. What may cause these oscillations is at this moment still unknown. However, it strongly suggests that there is a fault in the software with implementation of the random response analysis with CDTire/NVH in NVHD as the accelerometer response output was good but the interface force output is incomplete.

The final interior noise, presented in Section 5.4 also exhibits an oscillating behaviour, which may be due to the oscillations occurring at the interface forces. CDTire/NVH in NVHD is able to catch the peak in the rumble range well, however in the cavity range it does not capture any peak for 2.4bar pressure and only the lower one for 2.8bar. Furthermore CDTire/NVH in NVHD in general underestimates the interior noise compared to measurements and the spindle load method. From the results presented in Subsection 5.4.1 it can be clearly stated that there is something non-robust in the sensitivity with CDTire/NVH in NVHD. It is not physically reasonable that lowering the pre load of the car results in an increase of

10-15 dB in interior noise.

Interesting to note are the outcomes from previous related work. For example, Uhlar et. al. [2019] concludes that CDTire/NVH in NVHD predicts modal behaviour around 200Hz well for single tire cleat runs while in this project CDTire has shown weaknesses in predicting within the cavity range. Although they are different kinds of analyses in terms of single tire versus complete vehicle and cleat run versus road input, one could argue that the predictive capability should exhibit similarities between themselves. However, there are two significant differences between their assessment and this thesis. Firstly, they use CDTire/3D whereas CDTire/NVH is used in this project. Secondly the implementation of CDTire/3D is done in a MBS-tool in MSC.ADAMS while CDTire/NVH is implemented in NVHD. This raises questioning of CDTire/NVH and of the implementation in NVHD since something clearly goes wrong with either of these.

6.4 Delta study

The spindle load method shows strong similarities between 2.4 & 2.8 bar with 2.8 being slightly higher in some ranges and for the lower cavity peak. Even though the delta values differs in amplitude compared to the interior mic measurements, it still shows a similar trend over the frequency interval where 2.8 bar tends to be above 2.4 bar. CDTire shows a more varying delta between the pressures where there is no clear curve that obtains a higher level. Judging by these results, it is difficult to use CDTire to predict trends using different tire pressures.

6.5 Transfer Path Analysis

The fact that the methods are post processed in different software utilities creates difficulties evaluating the results as processes and computation behind presented values may differ. One difference is the inclusion of phase. CDTire accounts for phase where positive & negative contributions corresponds to in- & out-of-phase respectively while spindle load method does not account phase at all. Accounting of phase also enables contribution paths with CDTire to exceed 100% in contribution as both negative and positive contributions can occur. Reason why phase traditionally is not included in the spindle load method is to gain robustness as including phase increases sensitivity within the computation. Since the evaluation is on the methods as they are implemented, this is a difference that remains and is taken into account when evaluating.

In most cases CDTire predicts 2-4 out of five paths similar to the paths that are predicted by the spindle load method to be the highest contributors. Out of the two different pressures, predictions for 2.8bar performed more alike the spindle load method in comparison to a pressure of 2.4bar. Common for both pressures is that the highest contributors at the cavity peaks differs from the what the spindle load method predicts. However, as previously discussed that the CDTire is not able to

capture the cavity peaks properly, hence it follows that the correlation in the TPA results also may deteriorate. From a car development point of view, differences in important contributors raises the question of which method that is most reliable. Since the CDTire model still has difficulties with the cavity predictions in general it should, if necessary, only be used at lower frequencies to predict high contributors. However, looking at the overall performance of CDTire and the spindle load procedure, the results clearly shows that the spindle load method is more robust, reliable and performs better in comparison with CDTire.

6.6 General

Implementing and using CDTire/NVH in NVHD raised several issues as well as areas for improvement. CDTire/NVH in NVHD is still under development and the ability to extract all lines of data that the tires comes in contact with is not possible yet. Currently, road data can only be applied uniformly for each wheel. This means that the unevenness that can occur in the road across the width of the tire is not possible to capture as the full width of the tire experiences identical input road data. The consequence of this is that the input data for CDTire/NVH in NVHD differs slightly compared to what the other actual tire perceives during the measurements which may affect the results. However, whether this slight difference causes a significant effect or not is unknown but would be an interesting aspect for further analysis.

When setting up an analysis, previously created tire modules cannot be reused if a different car model is used, instead new ones must be created each time. As VCC's car models are defined in a negative x-direction, negative velocities for the tires are required. The consequences of defining negative velocities for the tires are something that should be thoroughly investigated to ensure that the analysis operates correctly regardless of sign in front the tire velocities. However this is an issue that the user cannot control but instead needs to be addressed by *Altair*.

Further issues with the analysis setup in NVHD is for example that certain analysis settings are not transferred from the GUI in the software to the *fem*-file but must instead manually be added in this file before submitting a job. With the job submitted, the computational performance of the model is also worth mentioning. Simulations performed with CDTire/NVH in NVHD takes about eight times longer compared with corresponding simulation using modal FE-models for the tire.

Post processing in NVHD has also proven to show weaknesses with version 2021.2 along with the integrated diagnostics utility. Whether this only applies for version 2021.2 or NVHD in general is unspoken of, as only 2021.2 has been used throughout this project. Reason for this is as mentioned that CDTire/NVH requires 2021.2 or newer, thereby, previous versions that may be more robust are not available. The software is inadequate in certain areas where bugs & errors causes additional struggle and effort to work around them. Furthermore, post processing includes parts where certain settings and selections must be executed in a certain sequence for it to work, otherwise the software ends up crashing. Aside from this, possible TPA options for

visualization is severely limited which further complicates post processing.

In general, a significant amount of errors and issues with the software exists where some of them also are quite fundamental. This causes further questioning of the software whether it is mature enough for being implemented in VCC's analysis procedure.

7

Conclusion

The aim was focusing on cavity noise predictions in particular, which the CDTire/NVH model as implemented in Altair NVH Director 2021.2 proved to have difficulties with. Furthermore, extensive issues with ripple in the results became apparent which raises questions regarding the stability of the overall analysis procedure using CDTire/NVH in NVHD. Hence, the general perception is that CDTire/NVH implemented in NVHD as of today does not fulfil the requirements of what is expected of a tire model, and the recommendation is thus to wait until a number of identified current bugs and errors in NVHD have been sorted out. In particular, the correlation and dependence of pre load and velocity needs to be investigated and clarified. The cause of the ripple in the results occurring at the interface points and interior mics needs to be sorted out and remedied. Additional TPA opportunities would also be preferable in order to not reduce the analysis possibilities currently available to VCC.

In addition to the deficits of the working procedure with the CDTire/NVH model, there are still great potentials that should be addressed. Among these, the potential of having a fully simulation-based approach without the requirement of a physical car in the development stage should be highlighted. In the lower frequency interval, CDTire/NVH in NVHD has actually proven to predict both absolute values and trends accurately relatively to the spindle load method. If the CDTire/NVH model implementation in NVHD undergoes an improvement of its predictive capability in the cavity region and the working procedure in NVHD is improved, there would be several benefits using CDTire models for road noise CAE procedures.

Bibliography

[Bäcker and Gallrein 2016] Bäcker, Manfred ; Gallrein, Axel: CDTire: Scalable tire model for full vehile simulations. In: *Fraunhofer ITWM* (2016)

[Cinkraut 2015] Cinkraut, Jakub: *Transfer Path Analysis of a Passenger Car*. Kungliga Tekniska högskolan, 100 44 Stockholm, Royal Institute of Technology, Diplom, 2015

[Gallrein et. al. 2018] Gallrein, A. ; Baecker, M. ; Guan, J: *Simulation of Dynamic Gas Cavity Effects of a Tire under Operational Conditions*. SAE Technical Paper, 2018

[ITWM 2022] ITWM, Fraunhofer: *CDTire/ 3D: Functional layer concept*. March 2022. – URL `https://www.itwm.fraunhofer.de/en/departments/mf/cdtire.html`

[O'Boy 2020] O'Boy, Daniel J.: Automotive wheel and tyre design for suppression of acoustic cavity noise through the incorporation of passive resonators. In: *Journal of Sound and Vibration* 467 (2020). – URL `https://doi.org/10.1016/j.jsv.2019.115037`

[OpenCRG 2022] OpenCRG, ASAM: *ASAM OpenCRG*. March 2022. – URL `https://www.asam.net/standards/detail/opencrg/`

[Park et. al. 2001] Park, J. ; Gu, P. ; Juan, J. ; Ni, A.: Operational Spindle Load Estimation Methodology for Road NVH Applications. In: *SAE Technical Paper* (2001). – URL `https://doi.org/10.4271/2001-01-1606`

[Parmar et. al. 2020] Parmar, Azan M. ; Mungara, Hari K. ; Miskin, Atul R. ; Himakuntla, Uma Maheswar R.: Advanced Diagnostics Simulations Approach For Random Response Analysis To Analyse Road NVH Characteristics. In: *INCE Conference Proceedings* (2020)

[Uhlar et. al. 2019] Uhlar, Stefan ; Heyder, Florian ; König, Thomas: Assessment of two physical tyre models in relation to their NVH performance up to 300 Hz. In: *Vehicle System Dynamics* 59 (2019), Nr. 3, S. 331–351. – URL `https://doi.org/10.1080/00423114.2019.1681475`

[Uhlar and Kunicky 2020] Uhlar, Stefan ; Kunicky, Zdenek: *Hybrid Simulation of Structure Borne Road Noise*. 2020

A

Accelerometer response

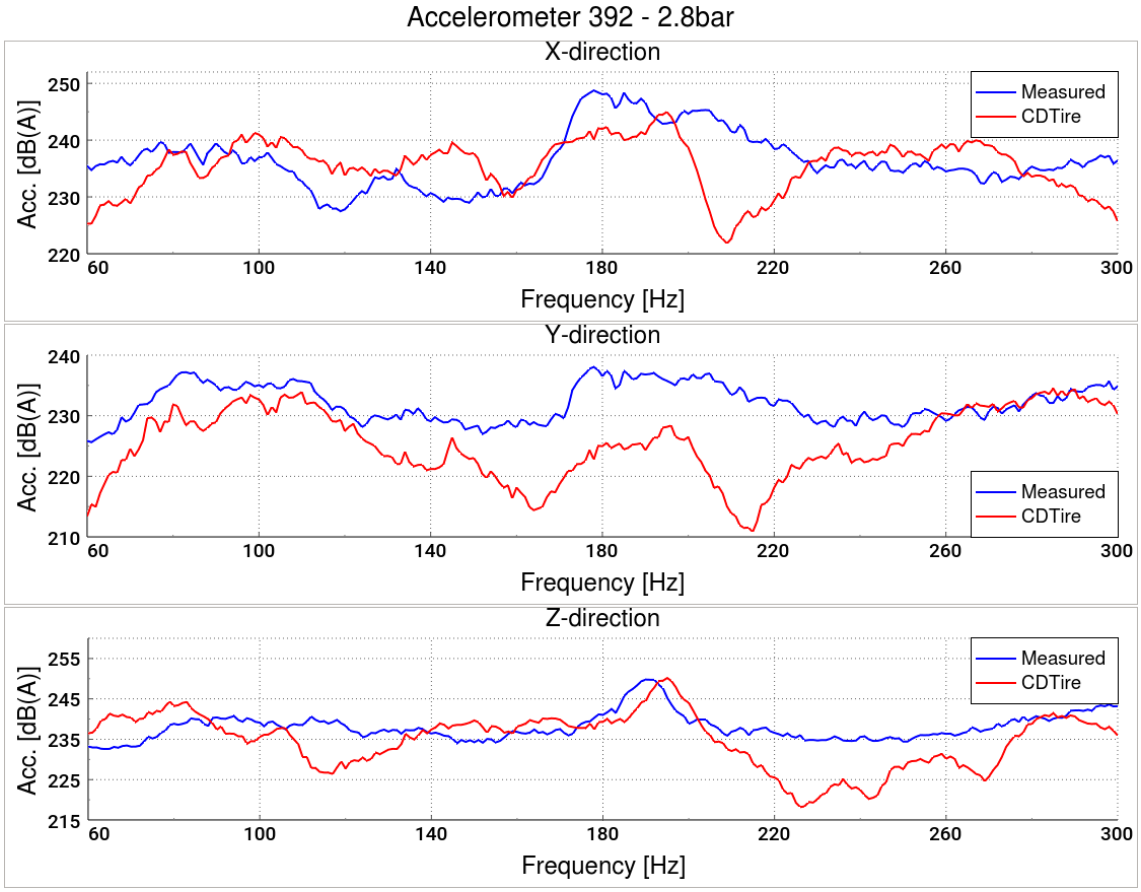

Figure A.2: Accelerations measured on accelerometer 392 for 2.8 bar

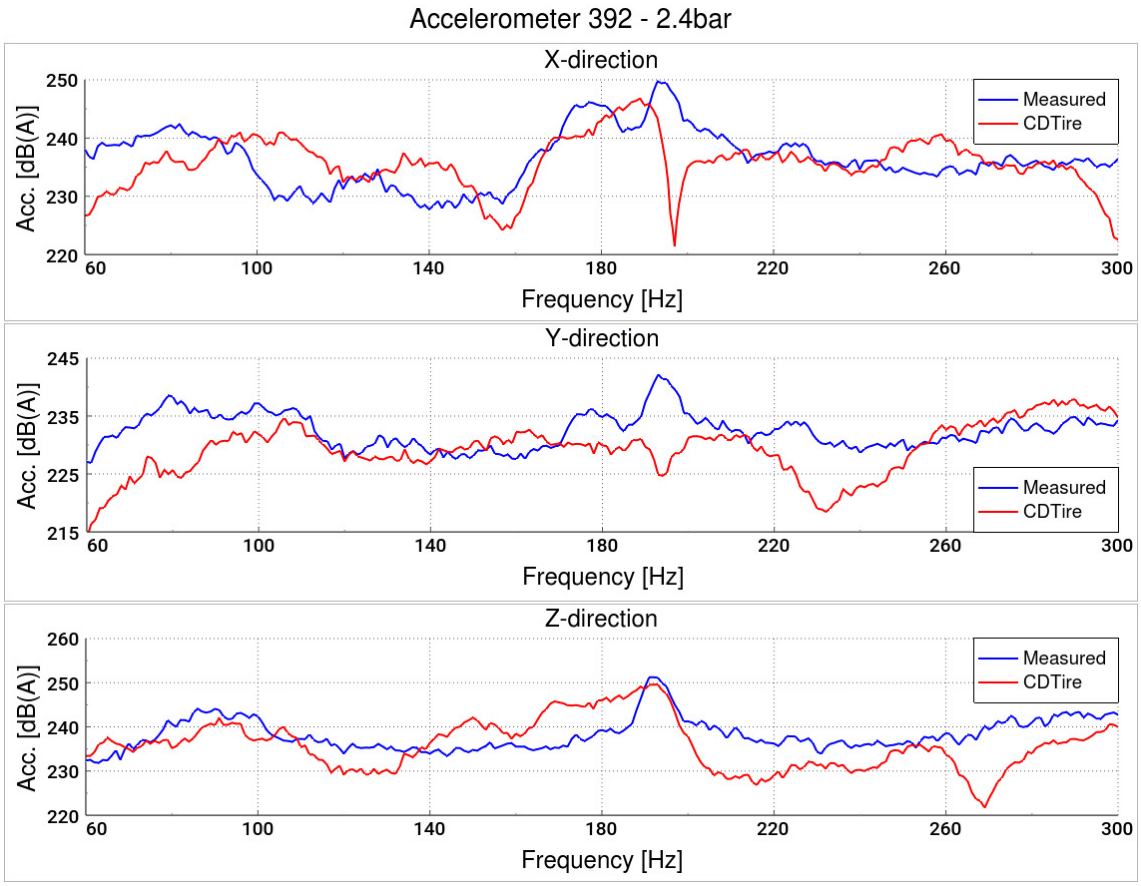

Figure A.1: Accelerations measured on accelerometer 392 for 2.4 bar

B

TPA analyses - 2.8bar

B.1 Rumble peak

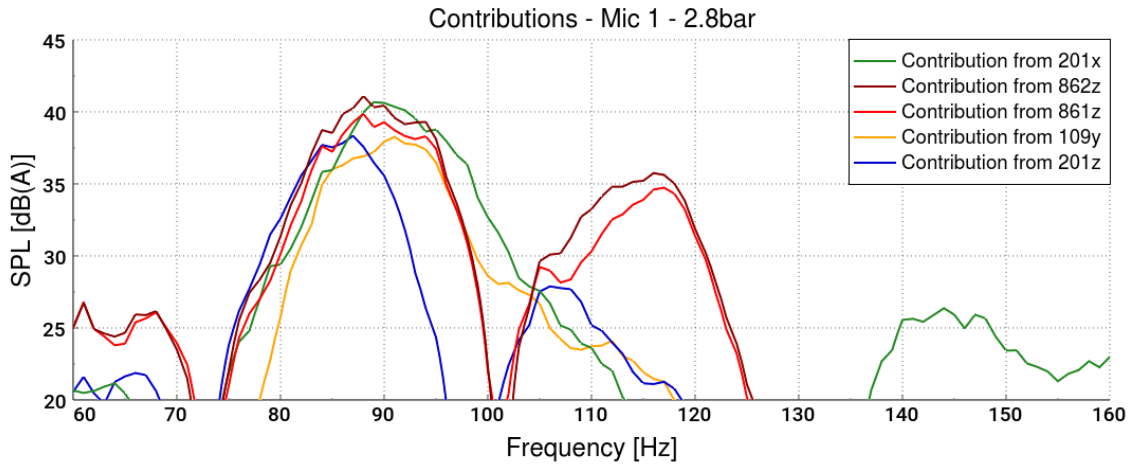

Figure B.1: Top five contributors in the rumble interval predicted by spindle load method at 2.8bar.

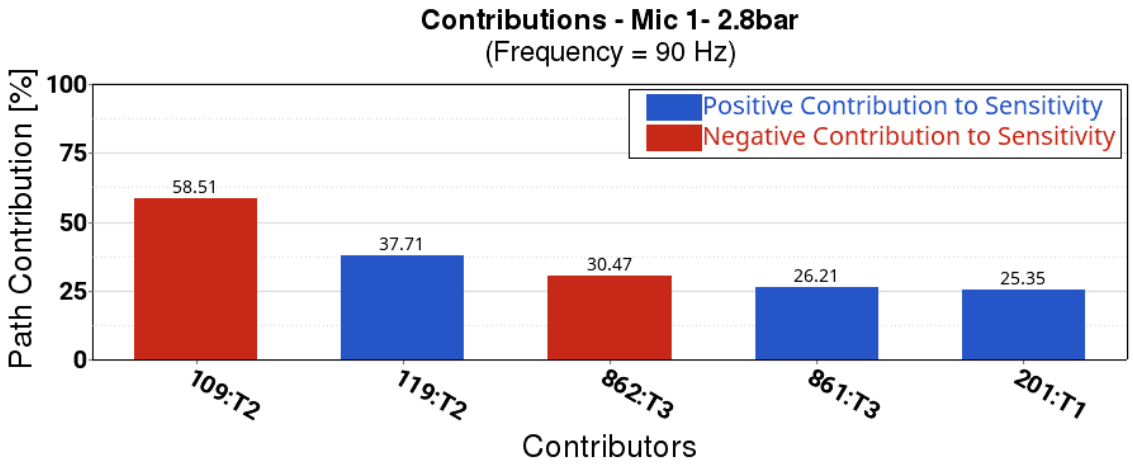

Figure B.2: Top five contributors at the rumble peak predicted by CDTire at 2.8bar.

B.2 Cavity peaks

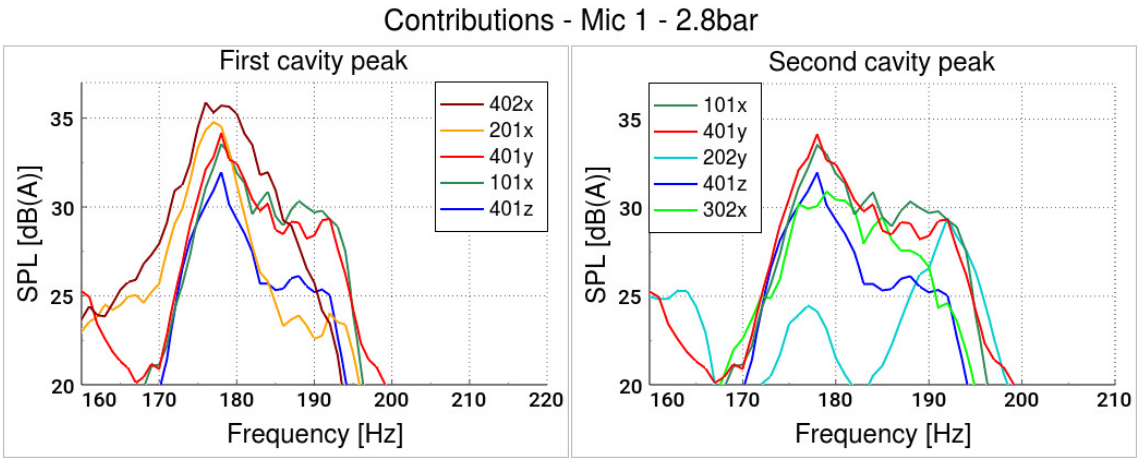

Figure B.3: Top five contributors in the cavity interval predicted by spindle load method at 2.8bar.

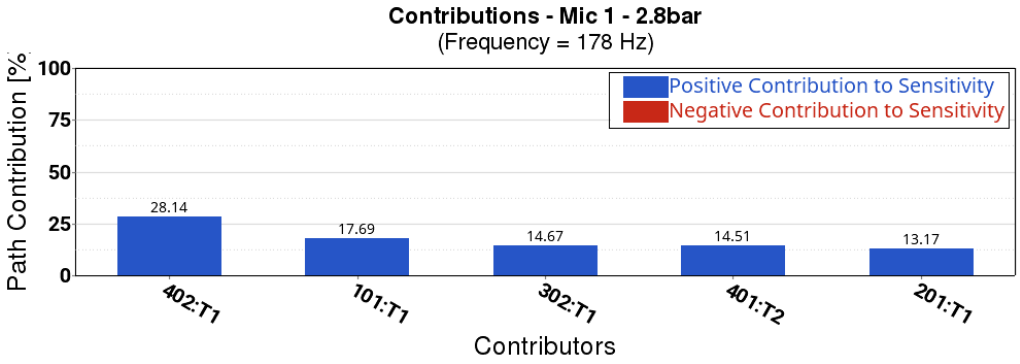

Figure B.4: Top five contributors at the first cavity peak predicted by CDTire at 2.8bar.

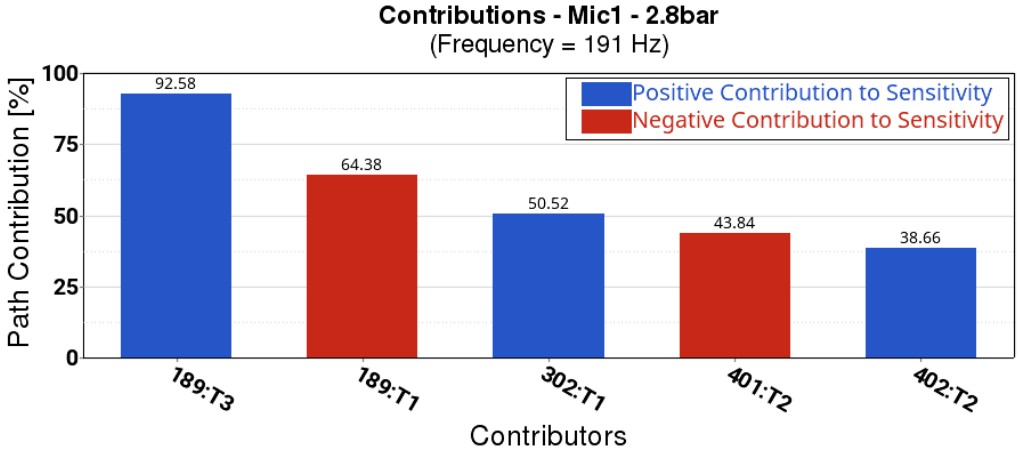

Figure B.5: Top five contributors at the second cavity peak predicted by CDTire at 2.8bar.

DEPARTMENT OF MECHANICS AND MARITIME SCIENCES
CHALMERS UNIVERSITY OF TECHNOLOGY
Gothenburg, Sweden
www.chalmers.se

CHALMERS
UNIVERSITY OF TECHNOLOGY